https://doi.org/10.1016/j.biomaterials.2023.122311

Gas station in blood vessels: an endothelium mimicking, self-sustainable nitric oxide fueling stent coating for prevention of thrombosis and restenosis

Jingdong Rao,[‡a,b] Xiaohui Mou,[‡c] Yongyi Mo,[a,b] Ho-Pan Bei,[a] Li Wang,[e] Chuyang Y. Tang,[e] Kai-Hang Yiu,[f] Zhilu Yang,*[c,d] Xin Zhao*[a,b]

a. Department of Biomedical Engineering, the Hong Kong Polytechnic University, Hung Hom, Kowloon, Hong Kong SAR, China.
b. Department of Applied Biology and Chemical Technology, the Hong Kong Polytechnic University, Hung Hom, Kowloon, Hong Kong SAR, China.
c. The Hong Kong Polytechnic University Shenzhen Research Institute, Shenzhen, China.
d. Affiliated Dongguan Hospital, Southern Medical University, Dongguan, Guangdong, China.
e. Guangdong Provincial Key Laboratory of Cardiac Function and Microcirculation, Guangzhou, Guangdong, China.
f. Department of Civil Engineering, the University of Hong Kong, Pokfulam Road, Hong Kong Island, Hong Kong SAR, China.
g. Cardiology Division, Department of Medicine, The University of Hong Kong, Queen Mary Hospital, Pokfulam Road, Hong Kong Island, Hong Kong SAR, China.
* Corresponding author: Dr. Xin Zhao, E-mail: xin.zhao@polyu.edu.hk; Prof. Zhilu Yang, E-mail: zhiluyang1029@smu.edu.cn
‡ These authors contributed equally

Abstract

Stenting is the primary treatment for vascular obstruction-related cardiovascular diseases, but it inevitably causes endothelial injury which may lead to severe thrombosis and restenosis. Maintaining nitric oxide (NO, a vasoactive mediator) production and grafting endothelial glycocalyx such as heparin (Hep) onto the surface of cardiovascular stents could effectively reconstruct the damaged endothelium. However, insufficient endogenous NO donors may impede NO catalytic generation and fail to sustain cardiovascular homeostasis. Here, a dopamine-copper (DA-Cu) network-

based coating armed with NO precursor L-arginine (Arg) and Hep (DA-Cu-Arg-Hep) is prepared using an organic solvent-free dipping technique to form a nanometer-thin coating onto the cardiovascular stents. The DA-Cu network adheres tightly to the surface of stents and confers excellent NO catalytic activity in the presence of endogenous NO donors. The immobilized Arg functions as a NO fuel to generate NO via endothelial nitric oxide synthase (eNOS), while Hep works as eNOS booster to increase the level of eNOS to decompose Arg into NO, ensuring a sufficient supply of NO even when endogenous donors are insufficient. The synergistic interaction between Cu and Arg is analogous to a gas station to fuel NO production to compensate for the insufficient endogenous NO donor *in vivo*. Consequently, it promotes the reconstruction of natural endothelium, inhibits smooth muscle cell (SMC) migration, and suppresses cascading platelet adhesion, preventing stent thrombosis and restenosis. We anticipate that our DA-Cu-Arg-Hep coating will improve the quality of life of cardiovascular patients through improved surgical follow-up, increased safety, and decreased medication, as well as revitalize the stenting industry through durable designs.

Keywords

Cardiovascular stent coating; anti-restenosis; anti-thrombosis; endothelium-mimicking; long-term nitric oxide production

1. Introduction

Cardiovascular disease (CVD) is the leading cause of disability and premature death.[1, 2] Plaque deposition, the accumulation of cellular debris, fatty substances, and connective tissue at the lesion site, are the major contributors of vascular blockage in CVD; its growth, calcification, and constriction of blood vessels eventually reduce blood flow.[3] Surgical intervention with cardiovascular stents (CVSs) is widespread to treat CVD with vascular obstruction.[4] However, stenting inevitably damages the endothelial structure, decreasing endothelial NO synthase (eNOS) activity and impairing NO production. This inability to maintain vascular homeostasis and ultimately exacerbates vascular obstruction by aggregated platelets and overgrown smooth muscle cells (SMCs).[5-7] Endothelial polysaccharide (such as heparin (Hep)) and nitric oxide (NO) produced by endothelial cells (ECs) maintain the anti-coagulant environment under physiological conditions.[8-10] Hep glycocalyx inhibits

fibrinogen/platelet adhesion and promotes NO production by increasing eNOS activity.[7, 11-13] Afterwards, the synthesized NO will feed back to EC to enhance migration/proliferation (re-endothelialization), and the activated NO-cyclic guanylate monophosphate (cGMP) pathway further inhibits platelet adhesion/activation (anti-thrombosis) as well as SMC migration/proliferation (anti-restenosis).[14, 15] That is, to prevent thrombosis and restenosis following stenting, it is essential to design an endothelium-mimicking vascular stent with NO-producing capabilities.

Recently, scientists have developed numerous NO-releasing/generating CVS coatings.[7, 16, 17] Due to its adhesive catechol structure, dopamine (DA) has been widely used in coating fabrication. For example, nanometer-thin dopamine-copper (DA-Cu) coatings with robust NO catalytic activity have been created.[17-19] Owing to the glutathione peroxidase (GPx)-like activity of Cu, these coatings are able to decompose endogenous S-nitrosothiols (RSNOs) into NO *in vitro* for more than 30 days.[19, 20] However, the coating designs often do not consider the low local concentration and short half-life of endogenous NO donors in actual pathophysiological microenvironments, so they may not support adequate NO catalyzing dosage *in vivo*. In patients with CVD, oxidative stress increases thioredoxin secretion, which accelerates the denitrosation and decomposition of endogenous RSNOs, resulting in a significant decrease in plasma RSNO concentration from 39 nmol/L (normal state) to 15 nmol/L (disease state).[21, 22] This poses a risk of insufficient NO generation from RSNOs *in vivo*, jeopardizing the long-term safety and efficacy of the coatings. Herein, in addition to incorporating NO catalyzing moieties into the CVS coating system, NO precursors should also be supplied to compensate for the potential reduction in RSNO levels in the actual pathophysiological microenvironment. As a naturally existing NO precursor *in vivo*, L-arginine (Arg) can generate NO via eNOS regardless of levels of endogenous RSNOs, ensuring adequate NO supply and NO storage.[23] Meanwhile, considering the disruption of endothelial structure and the impairment of eNOS, the introduction of glycocalyx Hep not only provides anticoagulant properties, but also increases the level of eNOS, thus facilitating NO production from Arg to maintain vascular homeostasis. Accordingly, incorporating Arg and Hep into the coating system is expected to prevent the systemic administration of RSNOs after stenting, reducing adverse effects such as vasodilation and hypotension.[24]

Here, a DA/hexamethylenediamine (HD)-Cu network with Arg and Hep

immobilization is used to produce an endothelium-mimicking, self-sustaining NO-fueling stent coating. In this system, DA adheres firmly to the stent surface via catechol interactions, while HD provides sufficient amino groups for surface grafting, establishing a solid foundation for biomolecule anchoring. DA and Cu form a coordination compound by complexation, where Cu can catalyze NO generation *in situ* by decomposing endogenous RSNOs. NO precursor Arg is covalently grafted to DA via Schiff base Michael addition, and releases NO under the influence of eNOS. Meanwhile, the grafted endothelial glycocalyx Hep enhances eNOS activity to facilitate NO production from Arg, forming a self-sustaining NO-producing and endothelium-mimicking stent coating and ensuring a sufficient and continuous supply of NO after stenting, even in the presence of low endogenous RSNOs (Fig. 1). This design enables each component of the DA-Cu-Arg-Hep coating to work complementarily and synergistically in endothelium reconstruction. From the aspect of coating stability, the DA-Cu base improves the hydrophilicity of the stent surface and provides abundant surface grafting sites. Then, the incorporation of Arg provides sufficient NO storage and the Hep modification enhances the hemocompatibility of the coating. From the aspect of coating function, Cu, Arg and Hep synergistically facilitate the NO production. Specifically, Cu acts as NO catalyzer, Arg serves as NO fuel, while Hep works as eNOS booster, and such supply chain compensates for the possible reduced levels of RSNOs in the actual pathophysiological microenvironment. Thus, this DA-Cu-Arg-Hep coating itself serves as a gas reactor to self-sustain NO production, fully fueling the regulation of vascular cell behavior without the need for additional input from the systemic administration of RSNOs. We anticipate that our DA-Cu-Arg-Hep coatings will promote re-endothelialization and inhibit platelet adhesion and SMC adhesion/proliferation/migration, and overcome the challenge of stent thrombosis and restenosis.

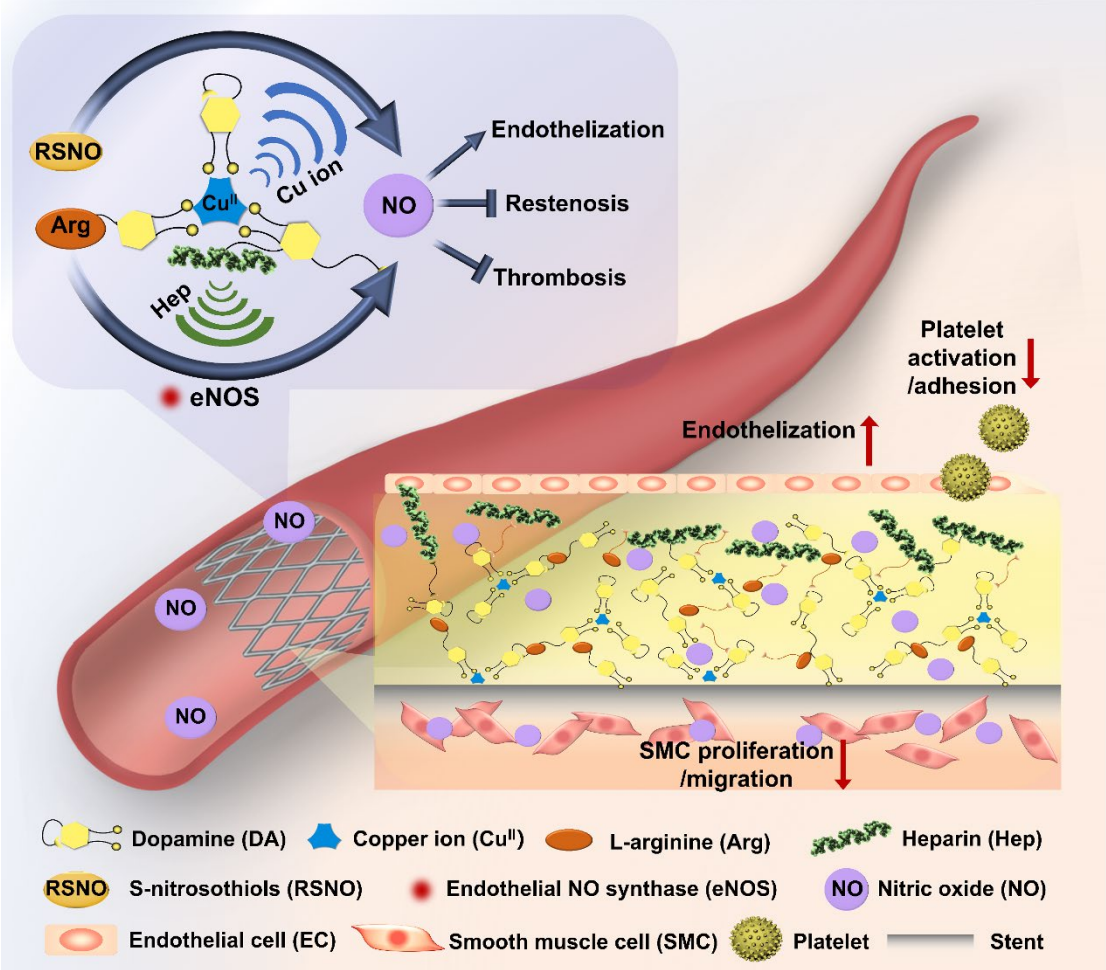

Fig. 1. A schematic illustrating the structure and function of an endothelium-mimicking, self-sustaining NO-fueling DA-Cu-Arg-Hep coating for cardiovascular stents. The proposed DA-Cu-Arg-Hep coating has a structure that resembles endothelium. The DA polymerizes and forms a network to allow sufficient Arg and Hep grafting, and Cu catalytically and continuously decomposes the endogenous NO donors (RSNOs) from the blood into NO. Meanwhile, Arg is converted to NO by eNOS whose activity can be upregulated by Hep. It compensates for the possibly diminished levels of RSNOs within the actual pathophysiological microenvironment. Such a combination of the DA-Cu network, Arg, and Hep reconstructs the endothelium structure and functions synergistically to ensure a sufficient, continuous, and self-sustainable supply of NO after stenting. In addition, it promotes EC migration and proliferation (a crucial role of endothelialization), inhibits platelet adhesion/activation/aggregation (a critical event in thrombosis), and SMC migration and proliferation (a significant factor contributing to restenosis), eventually enhancing re-endothelialization while inhibiting stent thrombosis and restenosis.

2. Materials and Methods

2.1 Materials

DA, HD, $CuCl_2 \cdot 2H_2O$, 2-(N-morpholino) ethanesulfonic acid hydrate (MES), N-hydroxysuccinimide (NHS), N-(3-dimethylaminopropyl)-N-ethylcarbodiimide (EDC), and S-Nitroso-Nacetylpenicillamine (SNAP) were purchased from Sigma-Aldrich, USA. Glutathione (GSH), Hep, and tris-(hydroxymethyl)-aminomethane hydrochloride (Tris-HCl) originated from Aladdin, China. Total NO assay kit, 3-Amino,4-aminomethyl-2',7'-difluorescein diacetate (DAF-FM DA) probe and NG-Monomethyl-L-arginine (L-NMMA) were supplied by Beyotime, China. FITC-Phalloidin, TRITC-phalloidin, 4',6-diamidino-2-phenylindole (DAPI), and cell counting kit-8 (CCK-8), Cell Tracker green and red were from Thermo Fisher, Hong Kong. cGMP enzyme linked immunosorbent assay (ELISA) Kit and eNOS ELISA Kit were from Elabscience, China. CD31 antibody and the FITC-secondary antibody was from Novus Biologicals, USA. Finally, human umbilical vein endothelial cells (HUVECs) were from ATCC, USA; human umbilical artery smooth muscle cells (HUASMCs) were from Otwobiotech, China; endothelial cell culture medium (ECM) and kit were from Sciencell, USA; and vascular smooth muscle cell medium and kit were from Otwobiotech, China.

2.2 Preparation of DA-Cu-Arg-Hep coatings

DA (1 mg/mL) and HD (2.44 mg/mL) were dissolved in pH 8.5 Tris-HCl (10 mM). $CuCl_2 \cdot 2H_2O$ (5 μg/mL) was then added to prepare a DA-Cu solution.[19] 316L SS foils and vascular stents were immersed in DA-Cu solution at room temperature for 24 h to prepare DA-Cu coatings onto the 316L SS substrates. Subsequently, the DA-Cu coated samples were immersed in a 1 mg/mL Arg solution (dissolved in PBS, pH 7.4) for 24 h to prepare the DA-Cu-Arg coatings.[17] Then, Hep (1 mg/mL) was preactivated by NHS (0.5 mg/mL) and EDC (1 mg/mL) in a 10 mg/mL MES (pH 5.5) solution for 20 min, and the DA-Cu-Arg samples were dipped into the above-stated activated Hep solution for 24 h and rinsed with ultrapure water.[7] The samples were ultraviolet (UV)-sterilized for 30 min.

2.3 Characterization of DA-Cu-Arg-Hep coatings

The chemical structure of the DA-Cu chelation was analyzed using the Matrix Assisted Laser Desorption/Ionization-Time of Flight Mass Spectrometer (MALDI-TOF, Bruker, Germany). Using X-ray photoelectron spectroscopy (XPS, Thermo Scientific NEXSA), the elemental composition of coating surfaces was determined. Using attenuated total reflection Fourier transform infrared spectroscopy (ATR-FTIR, Thermo Scientific NEXSA), the chemical structure of DA-Cu-Arg-Hep coatings was determined. Through scanning electron microscopy (SEM, Tescan VEGA3, Czech Republic), the surface morphology was examined. The mass of Arg immobilized onto the DA-Cu and Hep grafted onto the DA-Cu-Arg coating was determined using a quartz crystal microbalance with dissipation equipment (QCM-D, Q-sense AB, Sweden). Arg graft quantification was performed by inserting the coated samples into the QCM-D chamber and then injecting Arg solution into the QCM-D system. After saturation of Arg grafting, the samples were washed with PBS for 8 h to remove the weakly bound Arg and the residual Arg then indicated the Arg grafting amount. The final adsorbed mass was calculated according to the Sauerbrey equation. Similarly, for Hep quantification, the Hep solution was injected into the QCM-D system until the absorption was saturated, then the samples were washed with PBS for 8 h to remove the weakly bound Hep, and the final data were recorded to calculate the final adsorption mass. Using a spectroscopic ellipsometer (M-2000V, J.A. Woollam, USA), the coating thickness was measured. Water contact angle (WCA) was examined using a contact angle meter (OCA-20, Dataphysics Instruments, Germany) and calculated by the DSA 1.8 software to determine surface hydrophilicity at room temperature. A balloon dilation test was used to evaluate the mechanical stability of the coatings. The angioplasty balloon was connected to the DA-Cu-Arg-Hep-coated 316L SS cardiovascular stent. After the balloon was expanded for 1 min at 9 atm pressure, the expanded stent was examined by SEM to determine if the coating had any cracks.[18] Finally, the long-term stability of the DA-Cu-Arg-Hep coating under phosphate buffer saline (PBS) flow was performed by installing dilated DA-Cu-Arg-Hep stents into a polyvinyl chloride (PVC) tube and connecting it to a peristaltic pump with 200 mL/min PBS flush for 30 days. SEM was used to observe the surface morphology changes.

2.4 Evaluation of long-term NO production

To validate eNOS elevation effect of Hep and NO production effect of Arg, eNOS

inhibition test was carried out. Briefly, HUVECs were seeded at 5×10^4 cells/cm^2 on the coated samples in the medium with or without eNOS inhibitor L-NMMA (0.5 mM, supplemented every 24 h). After co-culture for 3 days, the eNOS level was measured by ELISA, the NO production was quantified by total NO kit and the NO signal was traced by DAF-FM DA probe. For long-term NO production, bare 316L SS, DA-Cu and DA-Cu-Arg-Hep coated foils (the coated samples were prepared as described in 2.2, where 1 mg/mL DA, 5 μg/mL $CuCl_2 \cdot 2H_2O$, 1 mg/mL Hep and 1 mg/mL Arg were used). All the samples were immersed at 37˚C in 1 mL of PBS (pH 7.4) containing NO donors (10 μM GSH and 10 μM SNAP, replaced every 6 h).[25-27] A total NO assay kit was used to quantify the long-term NO production for 1, 5, 10, 15, and 30 days. To examine the NO production from Arg, samples immersed in PBS at 0, 7, 14 and 28 days were removed, and HUVECs were seeded at 5×10^4 cells/cm^2 on each sample in the medium with or without NO donors (10 μM GSH and 10 μM SNAP) to evaluate the effect of Arg on NO production. The NO production at the cellular level was tracked using the DAF-FM DA probe, and the NO fluorescent signal was observed using a fluorescence microscope (DM2500, Leica, Germany).

2.5 Evaluation of adhesion, proliferation and migration of HUVECs and HUASMCs on the developed coatings

HUVECs or HUASMCs were seeded at 5×10^4 cells/cm^2 on bare and coated foils (DA, DA-Cu, DA-Cu-Arg, DA-Cu-Hep and DA-Cu-Arg-Hep coatings). The cells were then cultured either with or without NO donors (10 μM GSH and 10 μM SNAP, supplemented every 6 h). Live/dead staining was carried out to evaluate the cytotoxicity of the coatings. In brief, after co-culture of cells and samples with NO donors for 72 h, Calcein-AM and pyridine iodide (PI) solution was prepared by diluting the concentrates at a ratio of 1:1000 and 1:500 and incubation at 37°C for 20 min. The live (green) and dead (red) cells were observed using a fluorescence microscope. Samples were fixed with 4% paraformaldehyde and stained with FITC-phalloidin for fluorescence detection after 2, 24, and 72 h to examine cell adhesion and morphology. CCK-8 was used to assess cell proliferation on various coatings after 24 and 72 h of culture, and the results were normalized with respect to the amount of cells on the 316L SS group to obtain relative cell growth data.

To study the cell migration behaviors, the 316L SS foils (1.5 cm x 1.5 cm) were

folded in half vertically. Half of the foil was immersed in the reaction solution to form a coating on one side while the other remained uncoated. Before migration experiments, cells were seeded on one side of the semi-uncoated 316L SS surfaces and incubated for 4 h to ensure cell attachment. The side not covered by cells was then turned vertically and transferred to a new plate with fresh medium (NO donors were refreshed every 6 h), allowing the cells to migrate from the cell-covered side to the coating side. The samples were stained with FITC-phalloidin after 24 h. The cell migration was finally observed using a fluorescence microscope.[17]

2.6 Study on the competitive adhesion of HUVECs and HUASMCs on the developed coatings

By co-seeding these two cell types on the uncoated and coated surfaces, the competitive adhesion behaviors of HUVECs and HUASMCs were examined. Fluorescent cell trackers were pre-labeled with different colors to identify different cells. Green fluorescence was used to label HUVECs, whereas red fluorescence was used to label HUASMCs. The pre-labeled HUVEC and HUASMC suspensions were combined in equal volume and plated at 2×10^4 cells/cm^2 on uncoated and coated samples (DA, DA-Cu, DA-Cu-Arg, DA-Cu-Hep and DA-Cu-Arg-Hep coatings). After 24 and 72 h of culture (NO donors were replaced every 6 h), the cells on the samples were observed using a fluorescence microscope. The number of adhered cells was calculated from at least ten images using Image J software to determine the effects of different coatings on competitive adhesion of HUVECs and HUASMCs.[28]

2.7 Platelet adhesion assay

Fresh blood from male Sprague-Dawley rats (350-450 g) in good health was utilized. Blood collection was conducted following procedures approved by the Hong Kong Polytechnic University's Ethics Committee (18-19/70-BME-R-GRF). To verify the bioactivity of Hep, anti-Factor Xa (FXa) assay was performed following the guidance of the manufacturer. Briefly, platelet-poor plasma (PPP) was obtained by centrifugation of full blood under 3,000 rpm for 15 min, then the samples were incubated with 50 μL PPP at 37°C for 30 min. Afterwards, FXa testing reagents, including GENMED buffer, negative fluid and substrate solution, were added into each sample. After incubation for 60 min at 37°C, 100 μL of the supernatant was transferred to a new 96-well plate, and

absorbance was measured at 405 nm using a microplate reader. Afterwards, fibrinogen adsorption and activation were tested by measuring the level of fibrinogen (FN) and fibrinogen gamma chain (Fg-γ), respectively. Briefly, all the samples were incubated with 100 μL PPP with NO donors at 37°C for 2 h. The samples were then washed by PBS. For FN measurement, 100 μL of HRP labeled anti-rat fibrinogen was added and incubated at 37°C for 60 min, and then 50 μL chromogenic substrate 3,3′,5,5′-tetramethylbenzidine solution (TMB) was added and incubated for 10 min. The reaction was terminated by introducing quenching buffer and the absorbance was measured at 405 nm. Similarly, for Fg-γ measurement, 100 μL of HRP labeled anti-rat fibrinogen γ chain was added and incubated for 60 min, followed by the introduction of 50 μL TMB solution and color reaction termination by quenching buffer, and the absorbance was measured at 405 nm. For platelet observation, platelet-rich plasma (PRP) was obtained by centrifuging whole blood at 1,500 rpm for 15 min. The platelet count of PRP was 2.56×10^7 cells/mL and the PRP was diluted prior to seeding onto the surface of coated samples at 3×10^4 cells/well. The platelets were then incubated for 2 h at 37°C with NO donors. For adhesion observation, all samples were washed with PBS and preserved with 2.5% glutaraldehyde solution at 4°C overnight, followed by dehydration and dealcoholization with increasing ethanol concentrations (30, 50, 70, 90, and 100%). Each sample's platelet morphology was analyzed using SEM. To visualize platelet adhesion, Calcein-AM and PI were used to stain live and dead platelets respectively. Briefly, Calcein-AM and PI solution was prepared by diluting the concentrates at a ratio of 1:1000 and 1:500 and incubated at 37°C for 20 min. The platelets were observed by a fluorescence microscope and the number of adhered platelets was calculated using Image J software. To investigate the mechanism of anti-platelet effect, after 2 h of incubation with PRP, Triton-X was added followed by sonication. The mixture of co-incubation system was centrifuged at 2,500 rpm for 5 min, and the supernatant was collected and analyzed using a cGMP ELISA kit.[7, 29]

2.8 Underlying mechanism elucidation

To evaluate the possible mechanism and downstream signaling pathways influenced by DA-Cu-Arg-Hep coating, RNA sequence analysis was performed. Briefly, HUVECs were seeded at 5×10^4 cells/cm^2 onto bare and DA-Cu-Arg-Hep surface (supplemented NO donors every 6 h). After 3 days of incubation, total RNA of each group was

extracted by Trizol reagent. Afterwards, NEBNextRUltraTM RNA Library Prep Kit was used to prepare RNA-seq libraries, and the sequencing was performed using the Illumina hiseqx-10 platform. Gene Ontology (GO) enrichment and Kyoto Encyclopedia of Genes and Genomes (KEGG) analysis were performed using the cluster Profiler R package.[30]

2.9 Evaluation of the anti-thrombogenic efficacy *ex vivo* of the stent coatings

To further assess the anti-thrombogenicity of the developed coatings, an *ex vivo* rabbit arteriovenous (AV)-shunt model was established. Six male adult New Zealand white rabbits (3.5 - 4.0 kg) were used for this experiment, and each rabbit had 4 shunted PVC tubes (Fig. 6A), i.e., 4 parallels for each group. The *ex vivo* experiment was conducted according to procedures approved by the Ethics Committee of Affiliated Dongguan Hospital, Southern Medical University (K2022-01-011-014). Before the animal experiments, the bare, DA, DA-Cu, DA-Cu-Arg, DA-Cu-Hep and DA-Cu-Arg-Hep coated 316L SS foils were affixed into the wall of a commercial PVC blood transfusion system. After general anesthesia and barbering, the left carotid arteries and right jugular veins of rabbits were exposed. Then, their veins and arteries were connected to the blood transfusion system made from PVC. After 2 h of blood transfusion, the circuits were stopped, and the PVC tubes containing samples were fixed with a 2.5% glutaraldehyde solution for SEM analysis. Photographs of tube cross-sections were used to calculate the occlusion rate (original tube diameter minus final tube diameter divided by original tube diameter). Blood clots were additionally collected, photographed, and weighed.[31, 32]

2.10 Assessment of re-endothelialization and anti-restenosis efficacy *in vivo* of the stent coatings

An *in vivo* experiment was conducted according to procedures approved by the Ethics Committee of Affiliated Dongguan Hospital, Southern Medical University (K2022-01-011-014). Twenty-four male adult New Zealand white rabbits (3.5 - 4.0 kg) were used in the *in vivo* studies (four rabbits for 1 week, ten rabbits for 1 month and ten for 3 months). The rabbits were anaesthetized using 1% pentobarbital sodium and the iliofemoral arteries of the rabbits were exposed after being shaved. Commercial Primtech™ (bare 316L SS) stents and DA-Cu-Arg-Hep coated stents were implanted

in the opposite sites of the iliofemoral arteries. We observed that the surviving rabbits were able to move around, eat normally and were in a healthy state. After 1 week, 1 month, and 3 months of implantation, the stented arteries were harvested. Using CD31 fluorescence staining and SEM, each sample's endothelialization was monitored for 1 week. Each implanted sample was stained with Van Gieson's stain to examine the shape and form of the stented artery 1 and 3 months after implantation.[33, 34]

2.11 Statistical analysis

Unless otherwise stated, each experiment was conducted in triplicate. The data were presented using the mean ± standard deviation. T-test and one-way ANOVA were used to conduct statistical analysis using GraphPad Prism 8.0. $p < 0.05$, 0.01, and 0.001 were considered statistically significantly different, denoted with *, **, ***, respectively.

3. Results and Discussion

3.1 Chemical and physical properties of the DA-Cu-Arg-Hep coatings

The DA-Cu-Arg-Hep coatings on the surface of 316L SS (a material commonly used for CVS) were prepared by organic solvent-free three-dipping method in aqueous solution, avoiding the potential toxicity. The resultant 316L SS plates displayed a brown color, and SEM analysis revealed that all coated samples possessed uniform coating distribution (Fig. S1A). According to the energy-dispersed X-ray (EDX) data, all area contained Cu, S, C, N, and O peaks. The protuberant area had stronger elemental signals, while the flat area had less elemental distribution (Fig. S1B). Further MALDI-TOF-MS analysis was conducted to comprehend the potential polymerization between DA and Cu (Fig. 2A). The crosslinking reaction between DA and Cu was based on catechol and metal coordination, and peaks at 212, 335, and 610 m/z indicated the possibility of DA-Cu immobilization.[19] XPS was then used to analyze the elementary composition. As shown in Fig. 2B, DA-Cu and DA-Cu-Arg-Hep exhibited Cu peaks, demonstrating the successful coordination of Cu. In contrast to bare surface and DA-Cu coating, DA-Cu-Arg-Hep coating exhibited a distinct S peak (belongs to Hep). GATR-FTIR was further used to confirm the chemical structure of the DA-Cu-Arg-Hep coating. Fig. 2C demonstrated that both the DA-Cu and DA-Cu-Arg-Hep coatings had DA characteristic peaks relative to the uncoated samples, whereas the DA-Cu-Arg-Hep coating had a -C=N peak (~1700 cm^{-1}) and a -S=O peak (~1000 cm^{-1}), belonging to Arg and Hep,

respectively. QCM-D analysis was then used to quantify the grafting amount of Arg and Hep on the DA-Cu and DA-Cu-Arg bases in real-time. On the DA-Cu-coated and DA-Cu-Arg-coated surface, approximately 513 ± 11 ng/cm^2 Arg and 430 ± 28 ng/cm^2 Hep were grafted, as shown in Fig. 2D and Fig. 2E. These results demonstrate that the DA-Cu-Arg-Hep complexes successfully modified the 316L SS substrate.

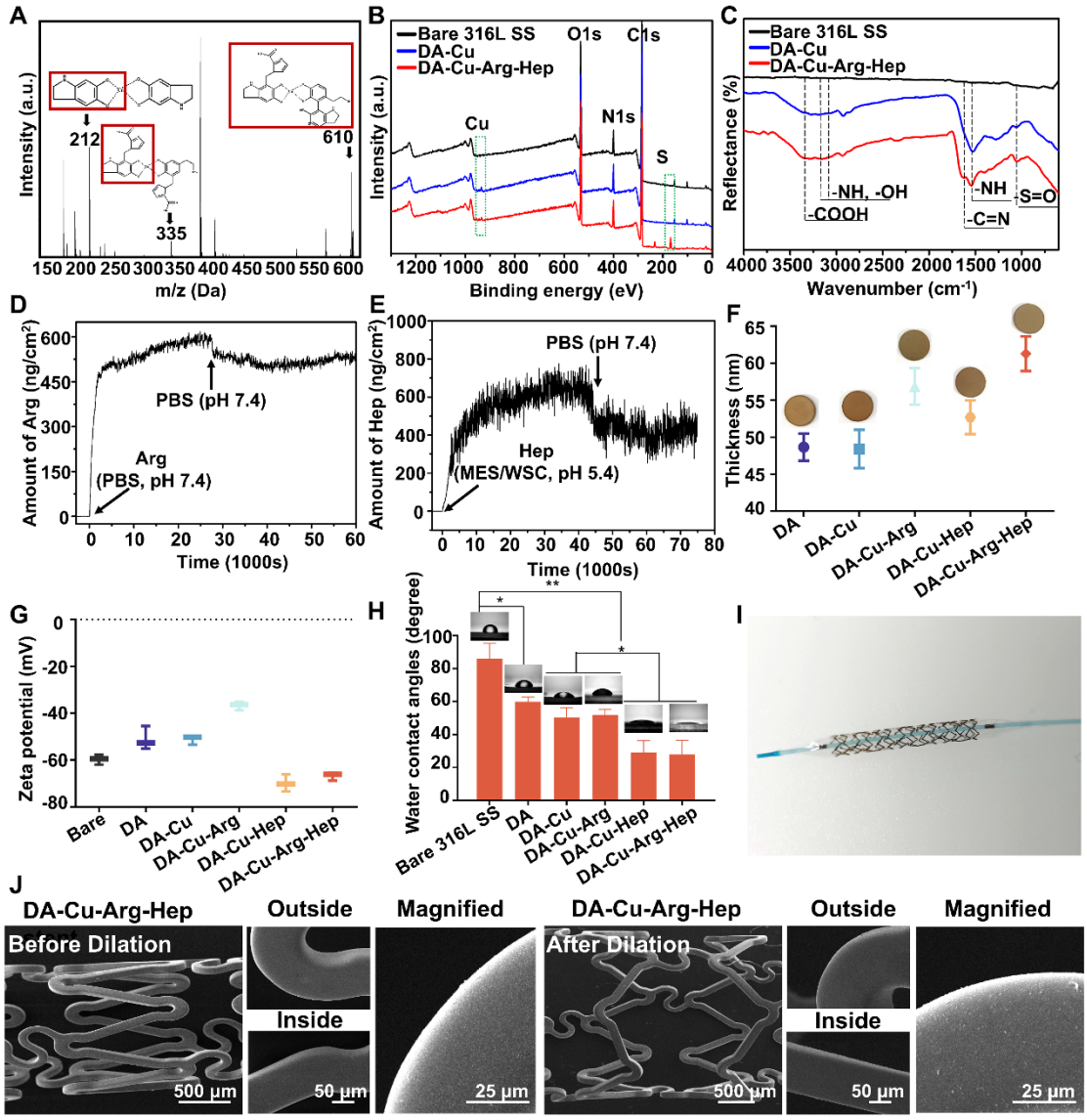

Fig. 2. Characterization of the DA-Cu-Arg-Hep coating. (A) MALDI-TOF-MS spectra of possible polymerization between DA and Cu. (B) XPS wide-scan survey spectra and (C) GATR-FTIR spectra of bare 316L SS, DA-Cu, and DA-Cu-Arg-Hep coatings. (D) Immobilization of Arg onto the DA-Cu coating using QCM-D. (E) Immobilization of Hep onto the DA-Cu-Arg surface using QCM-D. (F) Macroscopic observation of coated 316L SS substrates and thickness of each coating. (G) Zeta potential of the coated samples. (H) Water contact angles (WCA) of the bare and coated

samples. (I) A representative image of a DA-Cu-Arg-Hep coated stent with dilated angioplasty balloon. (J) Representative SEM micrographs of a DA-Cu-Arg-Hep-coated 316L SS stent before and after dilation.

Physical properties of the DA-Cu-Arg-Hep coating were then investigated. The thickness data (Fig. 2F) demonstrated that the coating became thicker after adding Arg and Hep, and the coating thickness ranged from 48 nm to 61 nm. This indicated that the DA-Cu-Arg-Hep coating was nano-thin, which was more stable than the micro-thickness and had minimal effect on the surface structure of the stent. Meanwhile, the zeta potential data (Fig 2G) presented a fluctuated tendency: the incorporation of Arg in the DA-Cu-Arg coating could elevate the zeta potential while the introduction of anionic Hep shielded the positive charge, indicating the DA-Cu-Arg-Hep had the potential to increase the endothelial homeostasis as cationic surface may adhere some macromolecules in blood. Subsequently, the WCA of each sample was measured.[17] As shown in Fig 2H, the bare 316L SS surface had extremely high WCA (~85.8°), whereas it was reduced (< 60°) for all DA-coated samples. This indicated that the immobilization of Cu, Arg, and DA increased the hydrophilicity of 316L SS bare stents. With the addition of Hep, the WCA of coated samples decreased dramatically to ~29°, which was attributed to the excellent hydrophilic properties of Hep. The increased hydrophilicity is conducive for cell adhesion and growth. The coated stents were then expanded with a balloon to evaluate the mechanical stability of the DA-Cu-Arg-Hep coating. SEM was used to observe the morphology of the dilated coated stents (to detect any crack formation) (Fig. 2I).[18] As depicted in Fig. 2J, the DA-Cu-Arg-Hep coating was homogeneous and compact before and after balloon dilation, with no visible cracks. To test the long-term stability of the DA-Cu-Arg-Hep coating under fluid flow, PBS was flushed through the stents for 30 days. As depicted in Fig. S2A, the coating was continuous and homogeneous without peeling after 30 days of PBS flush. Additionally, EDX spectroscopy (Fig. S2B) revealed that the DA-Cu-Arg-Hep coating still exhibited evident chemical element distribution (such as C, N, O, S, and Cu), demonstrating the coating's exceptional long-term stability. Collectively, these above results demonstrated the successful modification of the DA-Cu-Arg-Hep coating on the 316L SS substrates; such a coating was deformable and mechanically resistant to long-term fluid flow.

3.2 NO production from the DA-Cu-Arg-Hep coating

Due to the GPx-like activity of Cu in our prepared DA-Cu-Arg-Hep coating (Fig. 3A), it catalytically decomposes endogenous RSNOs into NO under the influence of GSH with the formation of a by-product glutathione disulfide (GSSG).[18] When endogenous NO donors are insufficient, adding Arg, a NO precursor, will increase the NO production and improve the cardiovascular function. In the presence of oxygen and nicotinamide adenine dinucleotide phosphate (NADPH), Arg will be converted to citrulline by eNOS, producing NO, which is expected to be elevated further by the grafted Hep. The elevated NO generation is conducive to EC proliferation.[31, 35] In addition, the produced NO can activate soluble guanylyl cyclase (sGC), and this interaction enables sGC to convert guanosine triphosphate (GTP) to cyclic guanylate monophosphate (cGMP).[36] Once cGMP is produced, various effects ensue, including SMC inhibition, anti-platelet adhesion, and vasodilation.[37] The self-sustaining NO fueling stent coating is anticipated to promote reendothelization and reduce thrombosis and restenosis. First, to verify the upregulation of eNOS by Hep and the NO production from Arg under eNOS, eNOS blocking experiments were carried out using NOS inhibitor L-NMMA.[38] As shown in Fig. S3A, eNOS was inhibited (black column) when L-NMMA was added, while significant eNOS upregulation was found in DA-Cu-Hep and DA-Cu-Arg-Hep containing groups (orange column) without L-NMMA. In Fig. S3B and C, the NO production was inhibited after eNOS suppression (black column). When eNOS inhibition was removed, DA-Cu-Arg and DA-Cu-Arg-Hep group could generate NO by Arg decomposition. Owing to the increased eNOS by Hep, DA-Cu-Arg-Hep had the highest NO amount. These experiments validated the eNOS upregulation effect of Hep, and NO production by Arg under the effect of eNOS. Afterwards, the long-term NO production was evaluated. Fig. 3B demonstrated that the bare samples had no obvious NO production, while both the DA-Cu and DA-Cu-Arg-Hep coatings initiated significant NO production in the presence of NO donors, with no significant difference between the two groups, confirming that Arg and Hep grafting did not affect the catalytic NO generation by Cu. After 30 days of immersion in PBS containing NO donors, the coated samples continuously produced NO and maintained approximately 50% of their initial NO production. As Arg can generate NO via eNOS in ECs, NO production at the cellular level was additionally measured without NO donors. Briefly, HUVECs were incubated on the sample surfaces without donors at

different time intervals. The quantitative results (Fig. 3C) demonstrated that in the absence of NO donors, the bare and DA-Cu samples could not produce NO, whereas the DA-Cu-Arg-Hep coating produced NO continuously by the synergistic effect of Arg and Hep. The NO signal could only be detected in the DA-Cu-Arg-Hep coating when the NO production was tracked with a fluorescent probe (Fig. 3D). The detected total NO surface flux rate of the DA-Cu and DA-Cu-Arg-Hep with NO donors were 3.139 and 4.082 × 10^{-10} mol/cm^2/min respectively, which were comparable to the physiological NO rate (0.5 - 4 × 10^{-10} mol/cm^2/min). As a result, such a DA-Cu-Arg-Hep coating is expected to promote endothelization and inhibit stent restenosis and thrombosis by enduringly releasing NO, with or without NO donors.

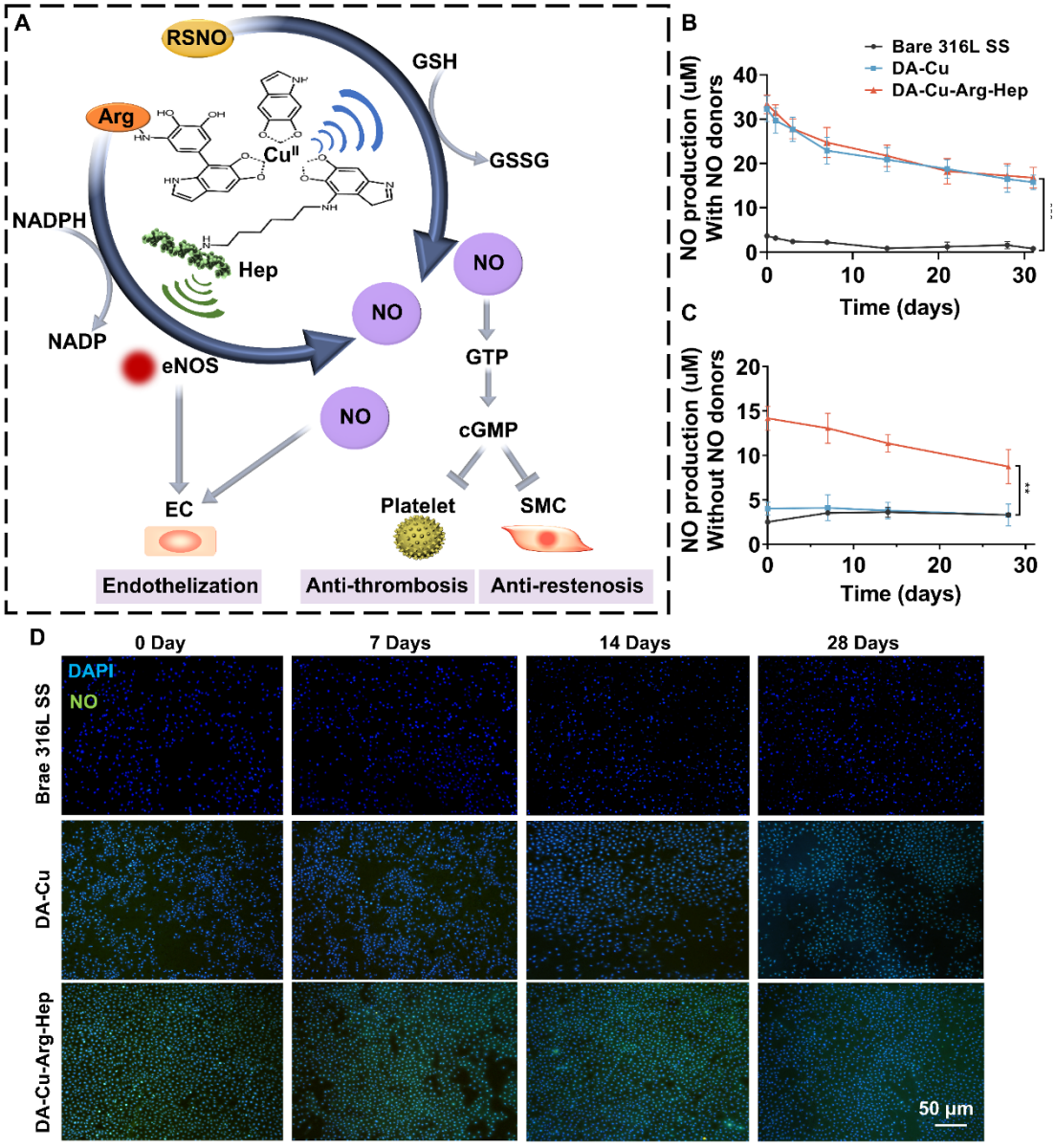

Fig 3. Long-term NO production from the DA-Cu-Arg-Hep coating. (A) Illustration

of self-sustained NO production from the DA-Cu-Arg-Hep coating and its effects on regulation of vascular cell behaviors. (B) Long-term NO generation by bare 316L SS, DA-Cu and DA-Cu-Arg-Hep coatings in the presence of NO donors. (C) Quantification of NO production in the absence of NO donors by bare 316L SS, DA-Cu and DA-Cu-Arg-Hep on HUVECs. (D) NO production in HUVECs (green signal) induced by bare 316L SS, DA-Cu and DA-Cu-Arg-Hep in the absence of NO donors at 0, 7, 14, and 28 days, as measured by the fluorescence probe DAF-FM DA.

3.3 Effects of coated samples on the growth behaviors of HUVECs and HUASMCs

3.3.1 Effect of coating on HUVEC adhesion/proliferation

The interaction between ECs/SMCs with their microenvironment is crucial for implanted cardiovascular stents.[39] Rapid regeneration of ECs on the surface of a stent facilitates re-endothelialization and the formation of a healthy endothelial layer.[40] In contrast, the overgrowth of SMCs induces extracellular matrix deposition, resulting in neointimal hyperplasia.[41] A desirable stent coating should be able to promote the growth of ECs but inhibit the proliferation of SMCs. As one of the primary components of the endothelium, NO and eNOS have been shown to support EC growth and inhibit SMC proliferation, which provides a unique advantage for the reconstruction of endothelium and the prevention of restenosis.[42, 43]

We thus analyzed the growth of HUVECs in each sample with and without NO donors. We found that in the absence of NO donors (Fig. S4A and B), the growth of HUVECs on uncoated, DA-coated, and DA-Cu-coated groups was restricted because Cu cannot catalytically generate NO in the absence of NO donors. The DA-Cu-Arg and DA-Cu-Hep groups exhibited enhanced proliferation, and the DA-Cu-Arg-Hep coating had the most potent effect due to the synergistic effect of Arg and Hep. In the presence of NO donors (Fig. 4A), the growth of HUVECs on the Cu-contained groups was enhanced compared to the bare and DA samples due to the catalytic NO production effect of Cu, and the DA-Cu-Arg-Hep group having the most potent effect on HUVEC growth promotion. At 72 h, the surface of DA-Cu-Arg-Hep was entirely covered by cells, and the quantitative data (Fig. 4B) demonstrated that the DA-Cu-Arg-Hep coating significantly increased the growth of HUVECs by 3.12-fold in comparison to the bare

samples. It demonstrates that the production of NO by Cu and Arg as well as the elevation of eNOS by Hep can stimulate the proliferation of HUVECs on the DA-Cu-Arg-Hep coating.

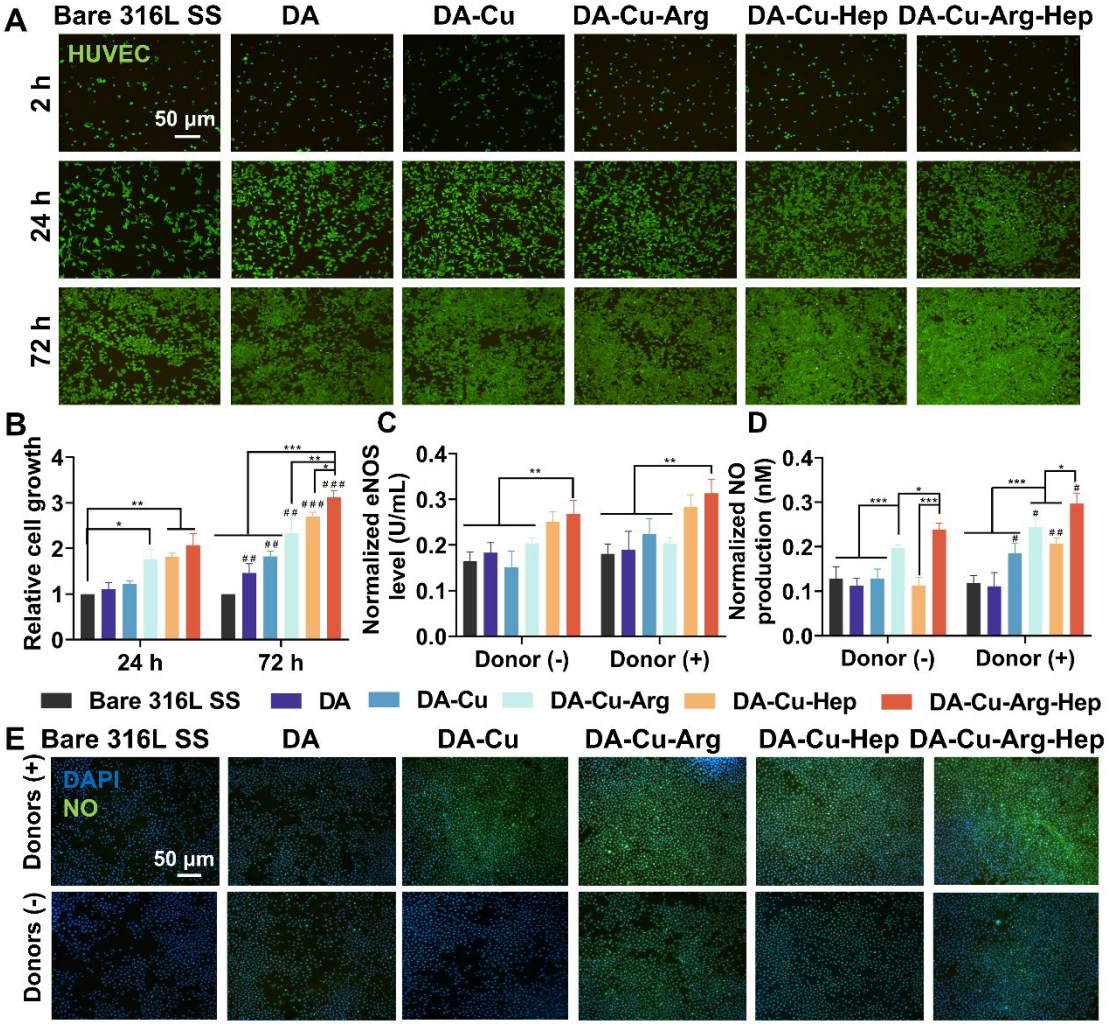

Fig 4. Growth behaviors of HUVECs on the DA-Cu-Arg-Hep coating with NO donors and the mechanism study. (A) Fluorescence images of HUVECs treated with NO donors for 2, 24, and 72 h, respectively. (B) Relative cell growth determined by CCK-8 assay after 24 and 72 h of culture. (C) The concentration of eNOS in HUVECs 72 h after exposure to NO donors. (D) Quantification of NO production in HUVECs incubated with or without NO donors for 72 h. (E) Fluorescence images demonstrating NO production in HUVECs with and without NO donors. *, ** and *** represent intra-group comparison, and $^{\#}$, $^{\#}$ and $^{\#\#\#}$ indicated inter-group comparison.

To verify the mechanism of increased EC growth, eNOS level and NO production

were evaluated. As an important functional protein of ECs, eNOS can promote the proliferation of ECs and convert Arg into NO, so increasing the expression of eNOS in HUVECs is highly advantageous.[23, 31] Fig. 4C shows the normalized eNOS level and NO production by cell number from the uncoated and coated surfaces. It demonstrated that the DA-Cu-Arg-Hep group significantly enhanced the eNOS level, increasing from 0.16 ± 0.02 U/mL (bare 316L SS) to 0.27 ± 0.03 U/mL (DA-Cu-Arg-Hep) without NO donor, and 0.18 ± 0.02 U/mL (bare 316L SS) to 0.32 ± 0.03 U/mL (DA-Cu-Arg-Hep) with NO donor. Although NO production could positively feed back to the level of eNOS, the difference between eNOS level with or without NO donors in the same group showed no significance after normalization, as the eNOS increase was mainly contributed by the presence of Hep. The NO production at the cellular level was further evaluated. Fig. 4D demonstrates that in the absence of NO donors, the DA-Cu-Arg-Hep coating could produce NO at 0.24 ± 0.01 nM with an evident green-fluorescence signal, indicating considerable NO production (Fig. 4E). In the presence of NO donors, the amount of NO in all Cu-containing coatings increased significantly, with the DA-Cu-Arg-Hep group having the highest fluorescence intensity and NO concentration (0.31 ± 0.02 nM), 2.05-fold higher than the bare group. Meanwhile, the mean fluorescence intensity of NO signal (Fig. S5) showed a similar trend that the DA-Cu-Arg-Hep coating could produce the highest amount of NO regardless of the presence of NO donor. Contributing to the synergistic NO production of Cu and Arg and the increased eNOS level, the DA-Cu-Arg-Hep coating ensured an EC-friendly microenvironment.

3.3.2 Effects of coating on HUASMC adhesion/proliferation

The adhesion and proliferation of HUASMCs to each sample were analyzed to study the SMC inhibitory effect. Without NO donors (Fig. S6A and B), HUASMCs grew well on each surface after 24 and 72 h of incubation. The growth of HUASMCs was slightly inhibited in the Hep-containing groups, as Hep has been reported to possess SMC-suppressing properties.[31] In the presence of NO donors, HUASMCs were attached to all substrates at 2 h (Fig. S7A). However, after 24 and 72 h of incubation, the growth of HUASMCs was significantly inhibited in the NO generation groups, with DA-Cu-Arg-Hep exhibiting the most potent inhibitory effect at 2.10-fold (24 h) and 2.27-fold (72 h) relative to the bare surface (Fig. S7B). The increased cGMP level brought about

by NO and Hep exemplifies the mechanism of SMC inhibition.[44-46] In Fig. S7C, the cGMP level was very low in the bare, DA, DA-Cu, and DA-Cu-Arg groups in the absence of NO donors, whereas the DA-Cu-Hep and DA-Cu-Arg-Hep groups exhibited elevated cGMP expression. In the presence of NO donors, all the Cu-containing coatings were found to elevate the cGMP level, which was highly correlated with the NO flux. The DA-Cu-Arg-Hep group displayed the highest cGMP expression, demonstrating its potent inhibitory effect on SMCs. These findings indicated that the DA-Cu-Arg-Hep coating could effectively inhibit HUASMC proliferation and intimal hyperplasia formation.

Furthermore, a live/dead staining of HUVECs and HUASMCs on each sample was performed to investigate the cytotoxicity of the developed stent coating, where green fluorescence was used to label living cells, and red fluorescence represented dead cells. As shown in Fig. S8, there was no obvious red fluorescence that appeared on the surface of stent coatings, which meant that the coatings had no obvious toxicity to cells, and the cell growth trend was consistent with that of the CCK-8 results (Fig. 4B and Fig S7B).

3.3.3 Effects of coating on HUVEC and HUASMC migration

Migration of ECs from adjacent endothelial tissue to the stent surface is essential for *in situ* re-endothelialization following stenting.[35] In contrast, inappropriate over-migration of SMCs can be harmful, frequently resulting in hyperplasia and in-stent restenosis after stent implantation.[47] In this regard, the migration distance of HUVECs and HUASMCs on various surfaces was measured. For HUVECs (Fig. S9A and B), fluorescence images revealed negligible cell migration on bare (26.60 ± 4.22 μm) and DA (41.25 ± 2.36 μm) surfaces. In contrast, the DA-Cu-Arg-Hep coating significantly increased cell motility (109.01 ± 5.87 μm) with NO donor supplements. For HUASMCs (Fig. S9C and D), the bare and DA surfaces exhibited only weak inhibition of HUASMC migration, with cells migrating 87.48 ± 7.54 μm and 71.54 ± 6.87 μm, respectively. In contrast, all NO generating groups improved the ability to inhibit the migration of HUASMCs, and the migration in DA-Cu-Arg-Hep (20.45 ± 1.27 μm) was reduced by 4.63-fold compared to the 316L SS alone. These results suggest that the DA-Cu-Arg-Hep would provide a biomimetic surface to promote EC migration from adjacent tissues while inhibiting SMC migration for healthy re-

endothelialization following stent placement.

3.3.4 Effects of coating on the competitive growth of HUVECs/HUASMCs

As the competitive growth of ECs and SMCs is essential for forming new endothelium and inhibiting restenosis, we investigated the effects of different coatings on the competitive growth of HUVECs/HUASMCs by co-seeding these two types of cells at a ratio of 1:1 on different samples while monitoring their fluorescence (green for HUVECs and red for HUAMSCs).[48] As shown in Fig. S10A, after 72 h of co-culture, the bare samples were predominantly covered by HUASMCs (red) and had few HUVECs (green). In contrast, the DA-Cu-Arg-Hep coating exhibited a strong green fluorescence with a diminished red signal, indicating the increased growth of HUVECs and the inhibition of HUASMCs. Fig. S10B demonstrated that the proliferation of HUVECs on the DA-Cu-Arg-Hep was significantly enhanced relative to SMCs at 72 h, and the ratio of HUVECs/HUASMCs increased from 0.504 ± 0.051 (bare 316L SS) to 1.814 ± 0.223 (DA-Cu-Arg-Hep), with 1.81-fold HUVEC enhancement and 2.11-fold HUASMC inhibition compared to the bare samples, demonstrating excellent selectivity for HUVEC growth. In conclusion, these results validate the superiority of the DA-Cu-Arg-Hep coating for generating a new endothelium and inhibiting SMC-induced restenosis.

3.4 Platelet adhesion

Before we evaluated the platelet adhesion, Hep bioactivity was tested. In general, active Hep will bind with FXa, which decreases the residual FXa level, hence the detection of FXa can reflect Hep activity.[49-52] The results (Fig. S11A) showed that the anti-FXa effect was enhanced after Hep grafting, and the absorbance of PPP co-incubated supernatant decreased from 1.028 (bare 316L SS) to 0.489 (DA-Cu-Hep) and 0.412 (DA-Cu-Arg-Hep), indicating the reduction of FXa and the Hep conjugated on the surface of DA-Cu-Hep and well-maintained bioactivity of DA-Cu-Arg-Hep. To investigate the antithrombotic function of the DA-Cu-Arg-Hep coating, fibrinogen adsorption assay was first carried out.[53, 54] The results showed that all samples had obvious fibrinogen adsorption, and the DA, DA-Cu, DA-Cu-Arg groups showed higher adsorption amount than the bare surface, which might be caused by the amino groups and increased surface roughness. In contrast, fibrinogen adsorption was decreased in the

DA-Cu-Hep and DA-Cu-Arg-Hep groups due to depletion of the amine groups by Hep grafting and the anticoagulant property of Hep. Afterwards, we performed fibrinogen activation assay. The results showed that both the bare and DA groups had high fibrinogen activation ability whereas the NO-producing groups reduced activation potential. We speculated that the NO might influence the protein conformation, thereby interfering activation process. Among all groups, the DA-Cu-Hep and DA-Cu-Arg-Hep groups showed the strongest inhibitory effect on fibrinogen activation, having a great potential to inhibit thrombosis.

After stenting, the initial cellular event potentially causing thrombosis is the rapid adhesion and aggregation of activated platelets at the implantation site; therefore, it is crucial to evaluate the antiplatelet properties of our newly developed coating.[31, 55, 56] As shown in Fig. S11D, neither the bare nor the DA substrates inhibited the adhesion of platelets. In contrast, the DA-Cu-Arg-Hep coating showed significant suppression of platelet adhesion with the NO donor supplement. To examine the effects of NO and Hep, the cGMP level in platelets on the bare and coated surfaces was measured (Fig. S11E). The coating of DA-Cu-Arg-Hep significantly increased the cGMP synthesis, corresponding to the decreased number of platelets on its surface. To further observe adherent platelets on each sample, live/dead assay was performed, where green fluorescence refer to live platelets and red signal represent dead platelets. The results (Fig. S11F and G) showed that the DA-Cu-Arg-Hep coating had least platelet adhesion, indicating DA-Cu-Arg-Hep has great anti-thrombotic potential. These results demonstrated the effectiveness of our proposed NO fueling coating in preventing thrombus formation on the surface of cardiovascular stents. *In vitro* experiments demonstrated that the DA-Cu-Arg-Hep coating selectively supported the EC proliferation/migration, suppressed SMC growth/migration, and inhibited platelet adherence/aggregation by its robust self-sustained NO production, promoting re-endothelization and inhibiting intimal hyperplasia and thrombosis.

3.5 Underlying mechanism evaluation

To reveal the underlying mechanism by which the DA-Cu-Arg-Hep coating affected HUVEC growth and endothelialization, we performed transcriptomic analysis of HUVECs cultured on the bare and DA-Cu-Arg-Hep surfaces. Pearson correlation analysis (Fig. S12A) shows that the correlation coefficients of all samples were larger

than 0.98, which was within the acceptable range (>0.92), suggesting that all the samples had satisfactory stability. Subsequently, the volcano plot (Fig. 5A) shows that 1430 genes were up-regulated, and 419 genes were down-regulated by the DA-Cu-Arg-Hep compared with the bare sample, revealing the coating-dependent changes in gene expression. Next, we performed the GO database evaluation using differential expression genes (DEGs), and the results shows that our proposed coating influenced many aspects including biological processes, molecular functions, and cellular components. Notably, the DA-Cu-Arg-Hep coating up-regulated many important genes that support endothelialization and angiogenesis such as EC adhesion, proliferation, migration and cell junction.

To explore the specific mechanisms of our proposed coating on cell behaviors, we performed KEGG pathway analysis based on these DEGs. Fig. 5B lists some pathways significantly regulated by the DA-Cu-Arg-Hep coating. Notably, pathways that are highly related to vascular endothelial health were influenced by our proposed coating, such as the mitogen-activated protein kinase (MAPK) pathway (relevant to NO mediated EC proliferation),[57, 58] the vascular endothelial growth factor (VEGF) pathway (key regulator for vascular development and re-endothelialization),[59, 60] Notch pathway (related to intimal hyperplasia in cardiology) [61-63] and Wnt pathway (coordinates with Notch pathway for normal vascular development).[64-66]

We then studied the specific gene expression to investigate how these pathways are influenced. The heatmap (Fig. 5C) shows that the DA-Cu-Arg-Hep coating decreased the level of some genes (such as DNAH8, SLC40A1 and IL33) that are involved in diseases (like huntington disease) or apoptosis. Meanwhile, genes favoring endothelial development were all upregulated, such as positive genes for both VEGF and MAPK pathways (SphK1 and PLA2G4C), a protective factor that prevents endothelial-mesenchymal transition (MAPK7), an activator of Wnt signaling and an inhibitor of Notch activity (Dvl).[68-71] Additionally, the ITPR3 gene associated with eNOS and NO was also activated, which favors blood vessel relaxation.[72, 73] Together, these results suggested that our DA-Cu-Arg-Hep coating could positively mediate EC behaviors through MAPK pathway, VEGF pathway and Wnt pathway, which was highly beneficial for shaping a healthy endothelial microenvironment.

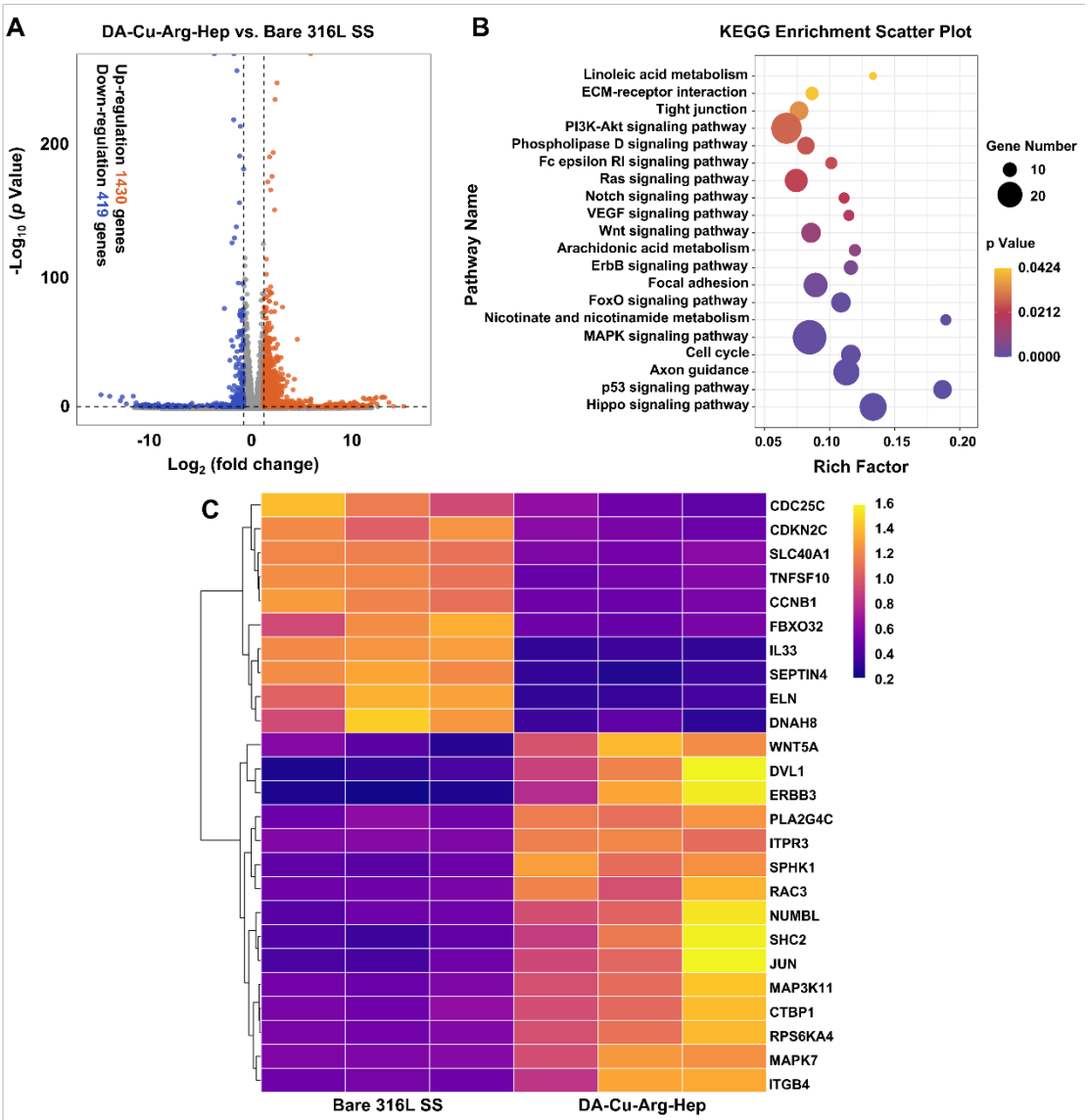

Fig. 5. Bioinformatic analysis of gene expression of HUVECs on bare 316L SS and DA-Cu-Arg-Hep samples. (A) Volcano plots of transcriptomic analysis. (B) GO classification of up-regulated genes. (C) Heatmap evaluation of DEGs (DA-Cu-Arg-Hep versus bare 316L SS).

3.6 *Ex vivo* anti-thrombogenic efficacy of DA-Cu-Arg-Hep coatings

An AV-shunt assay was used to investigate the antithrombotic properties of the developed coatings under blood flow.[42, 72] Briefly, the circuit connected the left carotid artery to the right external jugular to permit blood flow, while the samples were placed in the tubes' middle portion (Fig. 6A).[73, 74] After 2 h of *ex vivo* circulation, each group's thrombosis formation, occlusion, and blood flow rates were evaluated. As depicted in Fig. 6B, the uncoated 316L SS and DA cross-sections were entirely

occluded by blood clots, whereas there were reduced wall clots in other coated foils and the DA-Cu-Arg-Hep group had only a bare amount of thrombus on the wall. The SEM results (Fig. 6C) revealed many adhered platelets on the uncoated surface. In contrast, the number of platelets deposited on the coated surfaces decreased. The DA-Cu-Arg-Hep coating demonstrated the most significant platelet decrease due to the reduced thrombus formation. The occlusion rate (Fig. 6D) revealed that the bare and DA samples had an extremely high occlusion rate of 94.5 ± 2.5% and 93.7 ± 2.2%, respectively, while the DA-Cu-Arg-Hep samples had no discernible occlusion (7.4 ± 4.5%). Moreover, the thrombus weight in the DA-Cu-Arg-Hep group (10.46 ± 4.91 mg) was significantly less than that of the bare foils (58.32 ± 9.69 mg) (Fig. 6E). The decreased thrombus and occlusion facilitate the restoration of blood flow: the circuit of DA-Cu-Arg-Hep-coated foils had a higher blood flow rate (85.6 ± 6.3%) than the initial flow rate, significantly outperforming the bare foil at 10.1 ± 7.6% and DA at 11.5 ± 3.1%, while the blood flow in the DA-Cu-Arg-Hep coated foils were 1.48-fold, 1.60-fold and 1.35-fold higher than the DA-Cu, DA-Cu-Arg and DA-Cu-Hep, respectively (Fig. 6F). This indicates that the DA-Cu-Arg-Hep restored the most blood flow in the blood vessels toward normalcy. The DA-Cu-Arg was found to have a slightly greater occlusion and thrombus weight than the DA-Cu and DA-Cu-Hep. This could be due to the surface-exposed cations of the Arg. With the addition of Hep, the positive charge of Arg could be shielded, and the eNOS level could be increased to facilitate NO production from Arg, resulting in enhanced antithrombotic effects. Overall, the DA-Cu-Arg-Hep coating demonstrated superior antithrombotic, anti-occlusive, and blood flow restoration properties compared to the other groups.

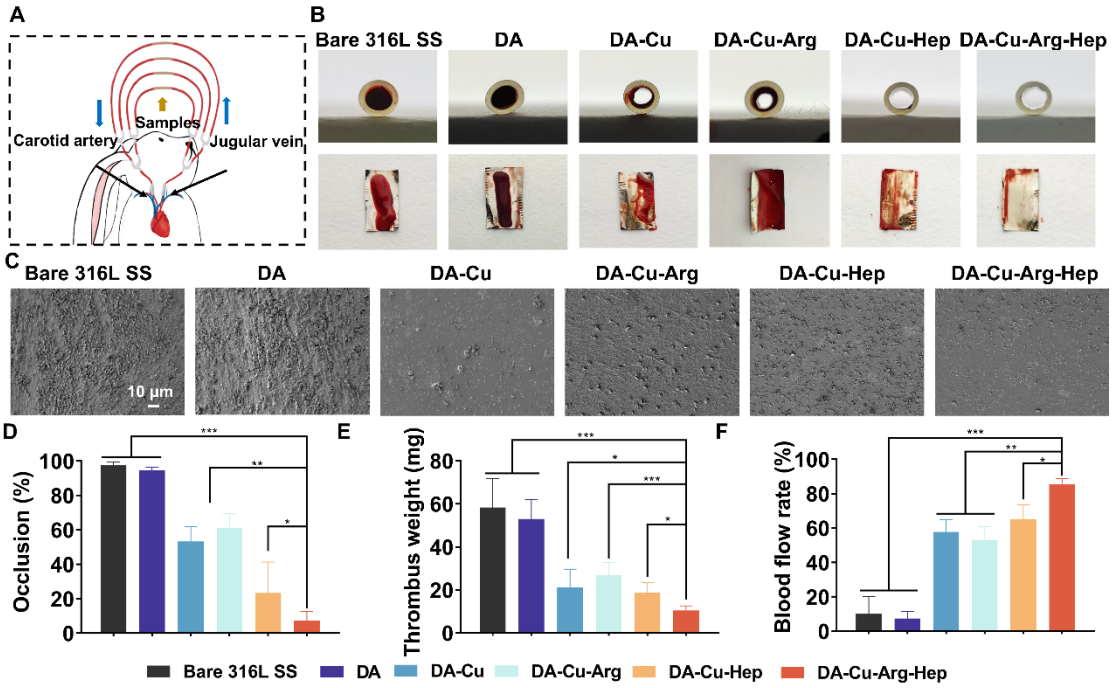

Fig. 6. Thrombogenicity of coated samples in a rabbit arteriovenous shunt (AV-shunt) model. (A) Diagram illustrating rabbit *ex vivo* circulation. (B) Photographs of tubes containing foils exposed to blood flow for 2 h. (C) SEM images of platelet adhesion. (D) Percentage of circuit occlusion and (E) thrombus weight. (F) Blood flow rate generated by various circuits after *ex vivo* circulation. (n=4)

3.7 *In vivo* re-endothelialization and anti-restenosis efficacy of DA-Cu-Arg-Hep coatings

To further investigate the effects of the DA-Cu-Arg-Hep coatings on re-endothelialization and anti-restenosis, rabbit iliofemoral arteries were implanted with coated stents.[75, 76] The SEM results at 1 week (Fig. 7A) confirmed the re-endothelialization of the DA-Cu-Arg-Hep stents, which was completely covered with a thin endothelium. In contrast, the control Primtech™ (a commercial bare 316L SS stent) exhibited limited endothelial coverage and apparent platelet adhesion on its surface. CD-31 immunofluorescence staining of the newly formed tissue was performed 1 week after implantation to verify endothelium coverage on the DA-Cu-Arg-Hep coating, where red fluorescence indicated cytoskeleton, green signal referred to ECs, and the blue signal was the cell nucleus (Fig. 7B). The results revealed discontinuous ECs on the Primtech™ stent. In contrast, the DA-Cu-Arg-Hep coated stents were completely covered by a continuous cell layer with a strong CD31 signal, confirmed by a newly formed endothelial layer. It indicates that the DA-Cu-Arg-Hep

coating provided a more favorable microenvironment for EC migration and proliferation. The DA-Cu-Arg-Hep stent's mean fluorescence intensity indicating CD31 signal (Fig. 7C), which was 2.35 times higher than that of the Primtech™ stent. These results demonstrated that the DA-Cu-Arg-Hep coating is capable of achieving rapid re-endothelialization.

Histomorphometric analysis was performed to investigate the anti-restenosis effect of the DA-Cu-Arg-Hep coated stents in greater detail (Fig 7D). At 1 month after implantation, the in-stent restenosis was not evident in these two groups; however, slight thickening was observed in the lumen of the Primtech™ stent, while the DA-Cu-Arg-Hep coated stents retained a distinct outline. At 3 months, the Primtech™ stents exhibited severe neointimal hyperplasia, whereas the DA-Cu-Arg-Hep coated stents exhibited significantly less restenosis. Mean neointimal area and stenosis percentage (Fig. 7E and F) were significantly reduced in the DA-Cu-Arg-Hep coated stents (0.80 ± 0.21 mm^2 and 14.12 ± 1.73%) compared to the Primtech™ stent (1.03 ± 0.14 mm^2 and 19.88 ± 4.35%) after 1 month. After 3 months of implantation, the mean neointimal area and stenosis percentage of the Primtech™ stents significantly increased to 3.09 ± 0.56 mm^2 and 47.37 ± 5.23%, respectively. In contrast, the DA-Cu-Arg-Hep coated stents possessed only 1.21 ± 0.24 mm^2 mean neointimal area and 23.69 ± 3.22% neointimal stenosis percentage. Taken together, these *in vivo* experimental results demonstrated that the DA-Cu-Arg-Hep-coated stents created a favorable microenvironment that supports stent re-endothelialization and reduces restenosis, preserving the long-term patency of CVSs.

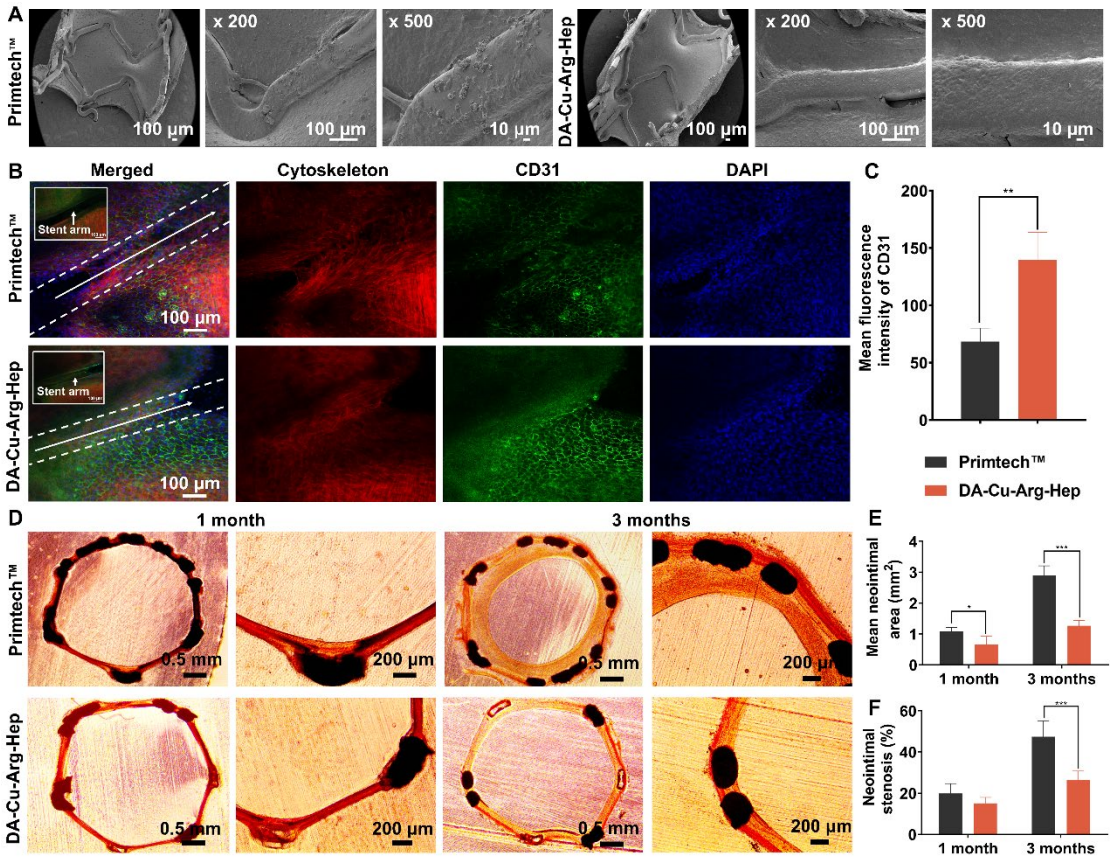

Fig. 7. Long-term re-endothelialization and anti-restenosis efficacy of the DA-Cu-Arg-Hep coatings. (A) Representative SEM images of implanted stents 1 week following implantation. (B) Fluorescent images of cytoskeleton (red by TRITC-phalloidin), CD31 (green by FITC-antibody) and cell nuclei (blue by DAPI) showing re-endothelialization of implanted stents 1 week after implantation. The DA-Cu-Arg-Hep stent was fully covered by a continuous green CD31 signal, indicating a great number of ECs grew on the stent surface, which had significant re-endothelialization effect. (C) The mean intensity of fluorescence of the CD31 signal. (D) Van Gieson's staining analysis of cardiovascular stent restenosis. (E) Neointimal area and (F) stenosis analysis of implanted stents (n=7).

4. Conclusion

In this study, we prepare a DA-Cu-Arg-Hep coating for cardiovascular stents using a three-dipping technique with no involvement of organic solvents. This stent coating combines Cu, Arg and Hep to produce NO synergistically under any condition. Specifically, with abundant endogenous RSNOs, Cu catalyzed the generation of NO;

without RSNOs, the coating is able to produce NO by decomposing Arg under the effect of eNOS, whose activity can be enhanced by Hep. Thus, this DA-Cu-Arg-Hep coating improves endothelial functions to ensure a sufficient and self-sustainable fueling of NO, regardless of the presence or absence of NO donors (Fig. S13). The DA-Cu-Arg-Hep coating was found to enhance the proliferation of ECs, suppressed SMCs, and decreased platelet adhesion. Further *ex vivo* and *in vivo* animal experiments demonstrated that the DA-Cu-Arg-Hep coating significantly improved blood and tissue compatibility, *in situ* re-endothelialization, anti-hyperplasia, and thrombus inhibition. Gene sequencing analysis demonstrates that the DA-Cu-Arg-Hep coating regulates several endothelial development-related pathways including the MAPK pathway, the VEGF pathway, the Notch pathway as well as the Wnt pathway. These results suggest that our coating represents a feasible and effective method to restore a healthy endothelium and to address stent thrombosis and restenosis. As far as we know, this is the first study to integrate Arg, Hep, and NO-generating moieties into a single CVS coating system using only simple, reproducible, and environmentally friendly procedures (no organic solvents involved) to fuel self-sustainable NO production. It facilitates mass production and widespread use in numerous settings, including public hospitals. This project provides a CVS coating strategy to prepare a biomimicking, self-sustainable CVS coating to persistently generate NO and prevent thrombosis and restenosis under any pathophysiological microenvironment (with or without the presence of sufficient endogenous RSNOs), potentially eliminating the need for systemic RSNO administration after stenting. It is highly advantageous, as systemic RSNO administration may cause adverse effects after stenting. Therefore, we believe that our DA-Cu-Arg-Hep coating can be widely applied in CVS, and the impact of the developed stent coatings on the quality of life of CVD patients will be immeasurable, including but not limited to decreased postoperative complications and reduced cost of medications such as extra NO donor supplementation and Arg administration.

Acknowledgement

This work was supported by the Innovation and Technology Fund of the Innovation and Technology Commission of Hong Kong (ITS/065/19), the National Natural Science Foundation of China and the Research Grants Council of Hong Kong Collaborative Research Scheme (N_PolyU526/22), the National Natural Science Foundation of China

(Project 82072072, 32171326), the International Cooperation Project by Science and Technology Department of Sichuan Province (2021YFH0056), and the High-level Talents Research and Development Program of Affiliated Dongguan Hospital (K202102), Guang Dong Basic and Applied Basic Research Foundation (2022B1515130010).

Authors' Contributions

X.Z. supervised the whole project. X.Z., Z.L.Y. and K.H.Y revised the manuscript. J.D.R. performed *in-vitro* experiments, analyzed the data and wrote the manuscript. X.H.M. performed animal experiments. Y.Y.M. helped with the platelet related experiments. H.P.B. wrote the manuscript. C.Y.Y.T. provided QCM-D equipment and L.W. performed QCM-D experiment. All authors approved this paper for publication.

Conflicts of interest

The authors declare no conflict of interest.

Data availability

The data used in the present study are available from the corresponding author on reasonable request.

References

[1] P. Joseph, D. Leong, M. McKee, S.S. Anand, J.D. Schwalm, K. Teo, A. Mente, S. Yusuf, Reducing the Global Burden of Cardiovascular Disease, Part 1: The Epidemiology and Risk Factors, Circ Res 121(6) (2017) 677-694.

[2] T.R. Frieden, M.G. Jaffe, Saving 100 million lives by improving global treatment of hypertension and reducing cardiovascular disease risk factors, J Clin Hypertens (Greenwich) 20(2) (2018) 208-211.

[3] T. Dave, J. Ezhilan, H. Vasnawala, V. Somani, Plaque regression and plaque stabilisation in cardiovascular diseases, Indian Journal of Endocrinology and Metabolism 17(6) (2013).

[4] J. Mehilli, J. Pache, M. Abdel-Wahab, S. Schulz, R.A. Byrne, K. Tiroch, J. Hausleiter, M. Seyfarth, I. Ott, T. Ibrahim, M. Fusaro, K.-L. Laugwitz, S. Massberg, F.-J. Neumann, G. Richardt, A. Schömig, A. Kastrati, Drug-eluting versus bare-metal stents in saphenous vein graft lesions (ISAR-CABG): a randomised controlled superiority trial, The Lancet 378(9796) (2011) 1071-1078.

[5] K.Y. Lo, C.K. Chan, Characteristics and outcomes of patients with percutaneous coronary intervention for unprotected left main coronary artery disease: a Hong Kong experience, Hong Kong Med J 20(3) (2014) 187-93.

[6] R. Sethi, C.H. Lee, Endothelial progenitor cell capture stent: safety and effectiveness, J Interv Cardiol 25(5) (2012) 493-500.

[7] Y. Yang, P. Gao, J. Wang, Q. Tu, L. Bai, K. Xiong, H. Qiu, X. Zhao, M.F. Maitz, H. Wang, X. Li, Q. Zhao, Y. Xiao, N. Huang, Z. Yang, Endothelium-Mimicking Multifunctional Coating Modified Cardiovascular Stents via a Stepwise Metal-Catechol-(Amine) Surface Engineering Strategy, Research (Wash D C) 2020 (2020) 9203906.
[8] A.C. Straub, A.W. Lohman, M. Billaud, S.R. Johnstone, S.T. Dwyer, M.Y. Lee, P.S. Bortz, A.K. Best, L. Columbus, B. Gaston, B.E. Isakson, Endothelial cell expression of haemoglobin alpha regulates nitric oxide signalling, Nature 491(7424) (2012) 473-7.
[9] R. Simon-Walker, R. Romero, J.M. Staver, Y. Zang, M.M. Reynolds, K.C. Popat, M.J. Kipper, Glycocalyx-Inspired Nitric Oxide-Releasing Surfaces Reduce Platelet Adhesion and Activation on Titanium, ACS Biomater Sci Eng 3(1) (2017) 68-77.
[10] S. Hauser, F. Jung, J. Pietzsch, Human Endothelial Cell Models in Biomaterial Research, Trends Biotechnol 35(3) (2017) 265-277.
[11] D.J. Suchyta, H. Handa, M.E. Meyerhoff, A Nitric Oxide-Releasing Heparin Conjugate for Delivery of a Combined Antiplatelet/Anticoagulant Agent, Molecular Pharmaceutics 11(2) (2014) 645-650.
[12] B. Wu, B. Gerlitz, B.W. Grinnell, M.E. Meyerhoff, Polymeric coatings that mimic the endothelium: combining nitric oxide release with surface-bound active thrombomodulin and heparin, Biomaterials 28(28) (2007) 4047-55.
[13] S. Weinbaum, J.M. Tarbell, E.R. Damiano, The structure and function of the endothelial glycocalyx layer, Annu Rev Biomed Eng 9 (2007) 121-67.
[14] T. Yang, Z. Du, H. Qiu, P. Gao, X. Zhao, H. Wang, Q. Tu, K. Xiong, N. Huang, Z. Yang, From surface to bulk modification: Plasma polymerization of amine-bearing coating by synergic strategy of biomolecule grafting and nitric oxide loading, Bioact Mater 5(1) (2020) 17-25.
[15] S. Yuan, C.G. Kevil, Nitric Oxide and Hydrogen Sulfide Regulation of Ischemic Vascular Remodeling, Microcirculation 23(2) (2016) 134-45.
[16] J. Rao, H. Pan Bei, Y. Yang, Y. Liu, H. Lin, X. Zhao, Nitric Oxide-Producing Cardiovascular Stent Coatings for Prevention of Thrombosis and Restenosis, Front Bioeng Biotechnol 8 (2020) 578.
[17] Q. Tu, X. Zhao, S. Liu, X. Li, Q. Zhang, H. Yu, K. Xiong, N. Huang, Z. Yang, Spatiotemporal dual-delivery of therapeutic gas and growth factor for prevention of vascular stent thrombosis and restenosis, Applied Materials Today 19 (2020).
[18] Z. Yang, Y. Yang, L. Zhang, K. Xiong, X. Li, F. Zhang, J. Wang, X. Zhao, N. Huang, Mussel-inspired catalytic selenocystamine-dopamine coatings for long-term generation of therapeutic gas on cardiovascular stents, Biomaterials 178 (2018) 1-10.
[19] F. Zhang, Q. Zhang, X. Li, N. Huang, X. Zhao, Z. Yang, Mussel-inspired dopamine-Cu(II) coatings for sustained in situ generation of nitric oxide for prevention of stent thrombosis and restenosis, Biomaterials 194 (2019) 117-129.
[20] Q. Tu, X. Shen, Y. Liu, Q. Zhang, X. Zhao, M.F. Maitz, T. Liu, H. Qiu, J. Wang, N. Huang, Z. Yang, A facile metal–phenolic–amine strategy for dual-functionalization of blood-contacting devices with antibacterial and anticoagulant properties, Materials Chemistry Frontiers 3(2) (2019) 265-275.
[21] C. Heiss, T. Lauer, A. Dejam, P. Kleinbongard, S. Hamada, T. Rassaf, S. Matern, M. Feelisch, M. Kelm, Plasma nitroso compounds are decreased in patients with endothelial dysfunction, J Am Coll Cardiol 47(3) (2006) 573-9.
[22] C. Gaucher, A. Boudier, F. Dahboul, M. Parent, P. Leroy, S-nitrosation/Denitrosation in Cardiovascular Pathologies: Facts and Concepts for the Rational Design of S-nitrosothiols, Current Pharmaceutical Design 19(3) (2012) 458-472.

[23] Y. Yang, T. Xu, Q. Zhang, Y. Piao, H.P. Bei, X. Zhao, Biomimetic, Stiff, and Adhesive Periosteum with Osteogenic-Angiogenic Coupling Effect for Bone Regeneration, Small 17(14) (2021) e2006598.
[24] Y.Y. Limin Liu, Ming Zeng, Jian Zhang, Martha A Hanes, Gregory Ahearn, Timothy J McMahon, Timm Dickfeld, Harvey E Marshall, Loretta G Que, Jonathan S Stamler, Essential roles of S-nitrosothiols in vascular homeostasis and endotoxic shock.pdf, Cell 116(4) (2004) 617-628.
[25] H. Wu, Q. He, L. Li, L. Li, Z. Zhou, N. Chen, M. Yang, Q. Luo, B. Zhang, R. Luo, L. Yang, Y. Wang, A facile and versatile superhydrophilic coating on biodegradable PLA stent with stepwise assembly of metal/phenolic networks for mimicking endothelium function, Chemical Engineering Journal 427 (2022).
[26] D. Wang, Y. Xu, L. Wang, X. Wang, S. Yan, G. Yilmaz, Q. Li, L.-S. Turng, Long-term nitric oxide release for rapid endothelialization in expanded polytetrafluoroethylene small-diameter artificial blood vessel grafts, Applied Surface Science 507 (2020).
[27] R. Luo, J. Zhang, W. Zhuang, L. Deng, L. Li, H. Yu, J. Wang, N. Huang, Y. Wang, Multifunctional coatings that mimic the endothelium: surface bound active heparin nanoparticles with in situ generation of nitric oxide from nitrosothiols, J Mater Chem B 6(35) (2018) 5582-5595.
[28] H. Qiu, P. Qi, J. Liu, Y. Yang, X. Tan, Y. Xiao, M.F. Maitz, N. Huang, Z. Yang, Biomimetic engineering endothelium-like coating on cardiovascular stent through heparin and nitric oxide-generating compound synergistic modification strategy, Biomaterials 207 (2019) 10-22.
[29] D. Suo, J. Rao, H. Wang, Z. Zhang, P.H. Leung, H. Zhang, X. Tao, X. Zhao, A universal biocompatible coating for enhanced lubrication and bacterial inhibition, Biomater Sci 10(13) (2022) 3493-3502.
[30] Y. Yang, T. Xu, H.P. Bei, L. Zhang, C.Y. Tang, M. Zhang, C. Xu, L. Bian, K.W. Yeung, J.Y.H. Fuh, X. Zhao, Gaussian curvature-driven direction of cell fate toward osteogenesis with triply periodic minimal surface scaffolds, Proc Natl Acad Sci U S A 119(41) (2022) e2206684119.
[31] B. Zhang, R. Yao, C. Hu, M.F. Maitz, H. Wu, K. Liu, L. Yang, R. Luo, Y. Wang, Epigallocatechin gallate mediated sandwich-like coating for mimicking endothelium with sustained therapeutic nitric oxide generation and heparin release, Biomaterials 269 (2021) 120418.
[32] H. Yu, S. Yu, H. Qiu, P. Gao, Y. Chen, X. Zhao, Q. Tu, M. Zhou, L. Cai, N. Huang, K. Xiong, Z. Yang, Nitric oxide-generating compound and bio-clickable peptide mimic for synergistically tailoring surface anti-thrombogenic and anti-microbial dual-functions, Bioact Mater 6(6) (2021) 1618-1627.
[33] H. Yu, H. Qiu, W. Ma, M.F. Maitz, Q. Tu, K. Xiong, J. Chen, N. Huang, Z. Yang, Endothelium-Mimicking Surface Combats Thrombosis and Biofouling via Synergistic Long- and Short-Distance Defense Strategy, Small 17(24) (2021) e2100729.
[34] X. Li, J. Liu, T. Yang, H. Qiu, L. Lu, Q. Tu, K. Xiong, N. Huang, Z. Yang, Mussel-inspired "built-up" surface chemistry for combining nitric oxide catalytic and vascular cell selective properties, Biomaterials 241 (2020) 119904.
[35] N. Lyu, Z. Du, H. Qiu, P. Gao, Q. Yao, K. Xiong, Q. Tu, X. Li, B. Chen, M. Wang, G. Pan, N. Huang, Z. Yang, Mimicking the Nitric Oxide-Releasing and Glycocalyx Functions of Endothelium on Vascular Stent Surfaces, Adv Sci (Weinh) 7(21) (2020) 2002330.
[36] L. Wen, S. Feil, M. Wolters, M. Thunemann, F. Regler, K. Schmidt, A. Friebe, M. Olbrich, H. Langer, M. Gawaz, C. de Wit, R. Feil, A shear-dependent NO-cGMP-cGKI cascade in platelets acts as an auto-regulatory brake of thrombosis, Nat Commun 9(1) (2018) 4301.
[37] M. Thunemann, K. Schmidt, C. de Wit, X. Han, R.K. Jain, D. Fukumura, R. Feil, Correlative intravital imaging of cGMP signals and vasodilation in mice, Front Physiol 5 (2014) 394.
[38] T. Xia, W. Guan, J. Fu, X. Zou, Y. Han, C. Chen, L. Zhou, C. Zeng, W.E. Wang, Tirofiban induces

vasorelaxation of the coronary artery via an endothelium-dependent NO-cGMP signaling by activating the PI3K/Akt/eNOS pathway, Biochem Biophys Res Commun 474(3) (2016) 599-605.
[39] J.L. Wang, B.C. Li, Z.J. Li, K.F. Ren, L.J. Jin, S.M. Zhang, H. Chang, Y.X. Sun, J. Ji, Electropolymerization of dopamine for surface modification of complex-shaped cardiovascular stents, Biomaterials 35(27) (2014) 7679-89.
[40] J. Yang, Y. Zeng, C. Zhang, Y.X. Chen, Z. Yang, Y. Li, X. Leng, D. Kong, X.Q. Wei, H.F. Sun, C.X. Song, The prevention of restenosis in vivo with a VEGF gene and paclitaxel co-eluting stent, Biomaterials 34(6) (2013) 1635-43.
[41] M. Alagem-Shafir, E. Kivovich, I. Tzchori, N. Lanir, M. Falah, M.Y. Flugelman, U. Dinnar, R. Beyar, N. Lotan, S.S. Sivan, The formation of an anti-restenotic/anti-thrombotic surface by immobilization of nitric oxide synthase on a metallic carrier, Acta Biomater 10(5) (2014) 2304-12.
[42] Z. Yang, X. Zhao, R. Hao, Q. Tu, X. Tian, Y. Xiao, K. Xiong, M. Wang, Y. Feng, N. Huang, G. Pan, Bioclickable and mussel adhesive peptide mimics for engineering vascular stent surfaces, Proc Natl Acad Sci U S A 117(28) (2020) 16127-16137.
[43] Z. Yang, Q. Tu, J. Wang, N. Huang, The role of heparin binding surfaces in the direction of endothelial and smooth muscle cell fate and re-endothelialization, Biomaterials 33(28) (2012) 6615-25.
[44] J.S. Pober, W.C. Sessa, Evolving functions of endothelial cells in inflammation, Nat Rev Immunol 7(10) (2007) 803-15.
[45] P. Gresele, S. Momi, G. Guglielmini, Nitric oxide-enhancing or -releasing agents as antithrombotic drugs, Biochem Pharmacol 166 (2019) 300-312.
[46] P.A. Cahill, E.M. Redmond, Vascular endothelium - Gatekeeper of vessel health, Atherosclerosis 248 (2016) 97-109.
[47] M.S. Kim, L.S. Dean, In-stent restenosis, Cardiovasc Ther 29(3) (2011) 190-8.
[48] H. Chang, K.F. Ren, J.L. Wang, H. Zhang, B.L. Wang, S.M. Zheng, Y.Y. Zhou, J. Ji, Surface-mediated functional gene delivery: an effective strategy for enhancing competitiveness of endothelial cells over smooth muscle cells, Biomaterials 34(13) (2013) 3345-54.
[49] T.R. Roberts, M.R.S. Garren, S.N. Wilson, H. Handa, A.I. Batchinsky, Development and In Vitro Whole Blood Hemocompatibility Screening of Endothelium-Mimetic Multifunctional Coatings, ACS Appl Bio Mater 5(5) (2022) 2212-2223.
[50] R. Devine, M.J. Goudie, P. Singha, C. Schmiedt, M. Douglass, E.J. Brisbois, H. Handa, Mimicking the Endothelium: Dual Action Heparinized Nitric Oxide Releasing Surface, ACS Appl Mater Interfaces 12(18) (2020) 20158-20171.
[51] Z. Zhou, M.E. Meyerhoff, Preparation and characterization of polymeric coatings with combined nitric oxide release and immobilized active heparin, Biomaterials 26(33) (2005) 6506-17.
[52] W.P.J. Jeanine M Walenga, Jawed Fareed, Short- and long-acting synthetic pentasaccharides as antithrombotic agents, Expert Opinion on Investigational Drugs 7(14) (2005) 847-858.
[53] K.-S. Park, S.N. Kang, D.H. Kim, H.-B. Kim, K.S. Im, W. Park, Y.J. Hong, D.K. Han, Y.K. Joung, Late endothelial progenitor cell-capture stents with CD146 antibody and nanostructure reduce in-stent restenosis and thrombosis, Acta Biomaterialia 111 (2020) 91-101.
[54] Y. Yang, X. Li, H. Qiu, P. Li, P. Qi, M.F. Maitz, T. You, R. Shen, Z. Yang, W. Tian, N. Huang, Polydopamine Modified TiO(2) Nanotube Arrays for Long-Term Controlled Elution of Bivalirudin and Improved Hemocompatibility, ACS Appl Mater Interfaces 10(9) (2018) 7649-7660.
[55] C. Chaabane, F. Otsuka, R. Virmani, M.L. Bochaton-Piallat, Biological responses in stented arteries, Cardiovasc Res 99(2) (2013) 353-63.

[56] C. Liang, Y. Hu, H. Wang, D. Xia, Q. Li, J. Zhang, J. Yang, B. Li, H. Li, D. Han, M. Dong, Biomimetic cardiovascular stents for in vivo re-endothelialization, Biomaterials 103 (2016) 170-182.
[57] A. Parenti, L. Morbidelli, X.L. Cui, J.G. Douglas, J.D. Hood, H.J. Granger, F. Ledda, M. Ziche, Nitric oxide is an upstream signal of vascular endothelial growth factor-induced extracellular signal-regulated kinase1/2 activation in postcapillary endothelium, J Biol Chem 273(7) (1998) 4220-6.
[58] A. Ptasinska, S. Wang, J. Zhang, R.A. Wesley, R.L. Danner, Nitric oxide activation of peroxisome proliferator-activated receptor gamma through a p38 MAPK signaling pathway, FASEB J 21(3) (2007) 950-61.
[59] G. Zeng, S.M. Taylor, J.R. McColm, N.C. Kappas, J.B. Kearney, L.H. Williams, M.E. Hartnett, V.L. Bautch, Orientation of endothelial cell division is regulated by VEGF signaling during blood vessel formation, Blood 109(4) (2007) 1345-52.
[60] K. Bujak, M. Lejawa, M. Gasior, T. Osadnik, The CTGF gene -945 G/C polymorphism is associated with target lesion revascularization for in-stent restenosis, Exp Mol Pathol 118 (2021) 104598.
[61] D.Y. Tian, X.R. Jin, X. Zeng, Y. Wang, Notch Signaling in Endothelial Cells: Is It the Therapeutic Target for Vascular Neointimal Hyperplasia?, Int J Mol Sci 18(8) (2017).
[62] P. Rizzo, L. Miele, R. Ferrari, The Notch pathway: a crossroad between the life and death of the endothelium, Eur Heart J 34(32) (2013) 2504-9.
[63] X. Zhou, X. Chen, J.J. Cai, L.Z. Chen, Y.S. Gong, L.X. Wang, Z. Gao, H.Q. Zhang, W.J. Huang, H. Zhou, Relaxin inhibits cardiac fibrosis and endothelial-mesenchymal transition via the Notch pathway, Drug Des Devel Ther 9 (2015) 4599-611.
[64] E. Dejana, The role of wnt signaling in physiological and pathological angiogenesis, Circ Res 107(8) (2010) 943-52.
[65] Y.C. Hsu, P.H. Lee, C.C. Lei, C. Ho, Y.H. Shih, C.L. Lin, Nitric oxide donors rescue diabetic nephropathy through oxidative-stress-and nitrosative-stress-mediated Wnt signaling pathways, J Diabetes Investig 6(1) (2015) 24-34.
[66] C. Caliceti, P. Nigro, P. Rizzo, R. Ferrari, ROS, Notch, and Wnt signaling pathways: crosstalk between three major regulators of cardiovascular biology, Biomed Res Int 2014 (2014) 318714.
[67] H. Bazzazi, A.S. Popel, Computational investigation of sphingosine kinase 1 (SphK1) and calcium dependent ERK1/2 activation downstream of VEGFR2 in endothelial cells, PLoS Comput Biol 13(2) (2017) e1005332.
[68] X. Wei, J. Wang, Y.Y. Deng, B.H. Shao, Z.F. Zhang, H.H. Wang, C.M. Wang, Tubiechong patching promotes tibia fracture healing in rats by regulating angiogenesis through the VEGF/ERK1/2 signaling pathway, J Ethnopharmacol 301 (2023) 115851.
[69] B. Vanchin, E. Offringa, J. Friedrich, M.G.L. Brinker, B. Kiers, A.C. Pereira, M.C. Harmsen, J.-R.A.J. Moonen, G. Krenning, MicroRNA-374b induces endothelial-to-mesenchymal transition and early lesion formation through the inhibition of MAPK7 signaling, The Journal of Pathology 247(4) (2019) 456-470.
[70] M. He, T.S. Huang, S. Li, H.C. Hong, Z. Chen, M. Martin, X. Zhou, H.Y. Huang, S.H. Su, J. Zhang, W.T. Wang, J. Kang, H.D. Huang, J. Zhang, S. Chien, J.Y. Shyy, Atheroprotective Flow Upregulates ITPR3 (Inositol 1,4,5-Trisphosphate Receptor 3) in Vascular Endothelium via KLF4 (Kruppel-Like Factor 4)-Mediated Histone Modifications, Arterioscler Thromb Vasc Biol 39(5) (2019) 902-914.
[71] Q. Yuan, J. Yang, G. Santulli, S.R. Reiken, A. Wronska, M.M. Kim, B.W. Osborne, A. Lacampagne, Y. Yin, A.R. Marks, Maintenance of normal blood pressure is dependent on IP3R1-mediated regulation of eNOS, Proc Natl Acad Sci U S A 113(30) (2016) 8532-7.

[72] P.G. Yin Chen, Lu Huang, Xing Tan, Ningling Zhou, Tong Yang, Hua Qiu, Xin Dai, Sean Michael, Qiufen Tu, Nan Huang, Zhihong Guo, Jianhua Zhou, Zhilu Yang & Hongkai Wu A tough nitric oxide-eluting hydrogel coating suppresses neointimal hyperplasia on vascular stent Nature Communications 12(1) (2021) 1-16.
[73] X. Mou, H. Zhang, H. Qiu, W. Zhang, Y. Wang, K. Xiong, N. Huang, H.A. Santos, Z. Yang, Mussel-Inspired and Bioclickable Peptide Engineered Surface to Combat Thrombosis and Infection, Research (Wash D C) 2022 (2022) 9780879.
[74] W. Wang, L. Lu, H.P. Bei, X. Li, Z. Du, M.F. Maitz, N. Huang, Q. Tu, X. Zhao, Z. Yang, Self-protonating, plasma polymerized, superimposed multi-layered biomolecule nanoreservoir as blood-contacting surfaces, Current Pharmaceutical Design 19 (2021) 458-472.
[75] M. Joner, A.V. Finn, A. Farb, E.K. Mont, F.D. Kolodgie, E. Ladich, R. Kutys, K. Skorija, H.K. Gold, R. Virmani, Pathology of drug-eluting stents in humans: delayed healing and late thrombotic risk, J Am Coll Cardiol 48(1) (2006) 193-202.
[76] C.C. Mohan, A.M. Cherian, S. Kurup, J. Joseph, M.B. Nair, M. Vijayakumar, S.V. Nair, D. Menon, Stable Titania Nanostructures on Stainless Steel Coronary Stent Surface for Enhanced Corrosion Resistance and Endothelialization, Adv Healthc Mater 6(11) (2017).